Universitetet i Stavanger

FACULTY OF SCIENCE AND TECHNOLOGY

MASTER'S THESIS

Study programme/specialisation: Petroleum Technology/Natural Gas Technology	Spring semester, 2019 Open
Author: Jørgen Hersve Thorød	…… (signature of author)
Programme coordinator: Kiyan Parham Supervisor: Kiyan Parham	
Title of master's thesis: Thermodynamic analysis of an ejector-absorption heat transformer utilizing H_2O-LiBr and a new working fluid H_2O-[EMIM][DMP]	
Credits: 30	
Keywords: Absorption Heat Transformer Ejector LiBr [EMIM][DMP] Energy Thermodynamic Analysis	Number of pages: 71 + supplemental material/other: 0 Stavanger, June 12. 2019

Abstract

The focus on human impact on the environment has increased within recent decades. Several large concerns regarding the threats to the stability of the environment have been brought up in public discussions. Amongst the greatest of these concerns are climate change. The public pressure on policy makers for combating climate change can perhaps be felt the easiest in the energy sector. Politicians, policy makers and consumers are looking to innovation and implementation of new technologies to aid the goals that have been set by numerous climate change agreements, most notably the Paris Agreement of 2016. In addition, a booming world population brings with it fast growing middle classes in developing countries, meaning that finding new methods for creating or improving energy production is of the utmost importance for the foreseeable future. One such method for improving upon the energy efficiency of pre-existing industries, or for better utilization of renewable energies is the implementation of absorption heat transformers. Absorption heat transformers is the second category of absorption heat pumps. It is a thermodynamic cycle, which can upgrade heat through an absorption process. This is done by taking in low to mid-grade waste heat from industry or from renewable energies such as geothermal heat or solar ponds and using a working fluid to drive an absorption reaction. It is based on an exothermic reaction which results in upgraded heat. The upgraded heat can be extracted and utilized in an array of different applications. These applications range from desalination to hydrogen production and energy recovery.

Across the decades, substantial research has gone into different types of working fluids and configurations of AHTs. Conventionally, working fluid pairs H_2O-LiBr or NH_3-H_2O have been used, but these have had problems such as crystallization in the case of LiBr, and toxicity and high pressures for NH_3. In recent years, research into the application of ionic liquids have been done to find replacements for the conventional solutions. Water and 1-Ethyl-3-methylimidazolium dimethyl phosphate or H_2O-[EMIM][DMP] is one such ionic liquid (IL) solution. Amongst new ways of configuring AHT cycles, adding an ejector before the absorber is one that has been investigated in the past. However, literature on

the subject is sparse, and studies done on an ejector-absorption heat transformer (EAHT) using IL solution has not been done yet.

The main objective of this thesis is to investigate the effect of adding an ejector to a single-stage absorption heat transformer using both H_2O-LiBr and H_2O-[EMIM][DMP] as the working fluids. For this purpose, a thermodynamic analysis is carried out, and the results are evaluated through the performance indicators of COP, ECOP, gross temperature lift, flow ratio and solution concentration difference. The working fluid crystallization risk is also investigated. The results are compared against the case without ejector by using graphs and tables. The thermodynamic analysis is carried out on Engineering Equation Solver (EES) from the perspective of the first law of thermodynamics (energy analysis).

The results indicated that [EMIM][DMP]-H_2O benefit more from the addition of ejector, having a superior performance increase compared to that of LiBr-H_2O. In fact, the performance of the system using LiBr-H_2O degraded over large portions of the investigated temperature ranges, only gaining an increase to its performance at high temperatures. But still, LiBr-H_2O continues to perform better than [EMIM][DMP]-H_2O generally when comparing the performances of both the two solutions against each other. The addition of ejector was found to be potentially helpful in lowering the crystallization risk of LiBr-H_2O, by allowing the system to start up at lower generator temperatures and substantially improving its performance at lower generator temperatures. To conclude, the addition of ejector is recommended generally for AHT systems.

Acknowledgements

I would like to thank Kiyan Parham and Mohammad Reza Kamali for their guidance and help throughout the semester. The completion of this thesis would not be possible without their help.

Table of content

Abstract 2
Acknowledgements 4
List of Figures 6
List of Tables 7
Nomenclature table 8
1 Introduction 9
1.1 Absorption heat transformers 10
2 Literature review 13
2.1 Working fluid pairs – refrigerant-absorbent: Conventional solutions 13
2.2 Working fluid pairs – refrigerant-absorbent: Alternative solutions 15
2.2.1 Alternative solutions: Ternary solutions 16
2.3 Working fluid pairs – refrigerant-absorbent: Ionic liquids 17
2.4 Ejector 20
2.4.1 Ejectors: Absorption refrigeration cycles 22
2.5 AHT applications 25
2.5.1 Desalination/Water purification 26
2.5.2 Energy recovery/conservation 27
2.5.3 CO2 capture improvement 29
3 Purpose of the study 30
4 Methodology 32
4.1 Systems description 32
4.2 Thermodynamic analysis of the ejector 35
4.3 Thermodynamic analyses of the systems 39
4.3.1 Performance indicators 40
4.3.2 Simulation basis 42
4.3.3 Thermodynamic properties 42
4.3.4 EMIM density confirmation 43
4.4 Model validation 45
5 Results and discussion 48
5 Conclusion 66
References 68

List of Figures

Figure 1.1 Simplified schematic of single-stage absorption heat transformer [19]. 11

Figure 2.1 Schematic diagram of an ejector-absorption heat transformer (EAHT) [20]..... 20
Figure 2.2 Schematic diagram of ejector used at entrance of the absorber [62]..... 24

Figure 4.1 Pressure - temperature diagram of the first system [34] 32
Figure 4.2 Schematic diagram of SAHT (S-Type I) [19]..... 33
Figure 4.3 Schematic diagram of ejection-absorption heat transformer (edited by author) [19]. 35
Figure 4.4 Schematic diagram of ejector used at entrance of the absorber (edited by the author) [62]. 36
Figure 4.5 Confirmation of EMIM density calculation working as intended plotted against experimental results from Gong et al. [74]. 44
Figure 4.6 Validation of the developed simulation model using H_2O-LiBr as working fluid pair (system 1) [55] 46
Figure 4.7 COP, ECOP and flow ratio as function of T_{abs}. For comparison to the values displayed for COP, ECOP and flow ratio of Shi et al. [55]. The values and behaviour of the three performance parameters are in good agreement here. Note the differing T_{abs} range..... 46
Figure 4.8 Validation of the developed simulation model using H_2O-[EMIM][DMP] as working fluid pair (system 2) [34, 47]..... 47

Figure 5.1 Effect of T_{gen} on COP and ECOP for both H_2O-LiBr and H_2O-[EMIM][DMP] cycles. (a) At T_{abs} = 120°C and T_{con} = 35°C. (b) At T_{abs} = 130°C and T_{con} = 35°C. (c) At T_{abs} = 110°C and T_{con} = 25°C. (d) At T_{abs} = 120°C and T_{con} = 25°C. 52
Figure 5.2 Effect of T_{abs} on COP for H_2O-LiBr cycle with and without ejector at various condenser temperatures..... 57
Figure 5.3 Effect of T_{abs} on ECOP for H_2O-LiBr cycle with and without ejector at various condenser temperatures..... 57
Figure 5.4 Effect of T_{abs} on COP for H_2O-[EMIM][DMP] cycle with and without ejector at various condenser temperatures..... 59
Figure 5.5 Effect of T_{abs} on ECOP for H_2O-[EMIM][DMP] cycle with and without ejector at various condenser temperatures..... 60
Figure 5.6 Effect of T_{abs} on COP for H_2O-LiBr cycle with and without ejector at various evaporator temperatures..... 62
Figure 5.7 Effect of T_{abs} on COP for H_2O-[EMIM][DMP] cycle with and without ejector at various evaporator temperatures..... 62
Figure 5.8 Effect of T_{abs} on Δx and flow ratio for H_2O-LiBr and H_2O-[EMIM][DMP]..... 64
Figure 5.9 Effect of condenser and heat source temperature on H_2O-LiBr crystallization with ejector, compared against H_2O-[EMIM][DMP]. Original plot by Kamali et al. [34], modified by author for ejector and addition of system 2..... 65

List of Tables

Table 2.1 Summary of single-stage absorption heat transformer presented section 2.1 - 2.3 19
Table 2.2 Summary of exergy loss in the different components [57] 22

Table 4.1 Regression parameters used in density equation 43

Table 5.1 The input parameters of the simulation 48
Table 5.2 Comparison of outputs of both systems with and without ejector at defined input parameters 53
Table 5.3 State properties of the streams of the cycles at reference operating condition 54
Table 5.4 GTL comparison between system with ejector and without ejector 61

Nomenclature table

AHT	absorption heat transformer	*Subscripts*	
EAHT	ejector absorption heat transformer	*0*	reference conditions
A	area, m^2	*gen*	generator
COP	coefficient of performance	*eva*	evaporator
ECOP	exergetic efficiency	*abs*	absorber
D	diameter, m	*con*	condenser
V	velocity, m s^{-1}	*N*	nozzle
P	pressure, kPa	*M*	mixing section
$\dot{m}$	mass flow rate, kg s^{-1}	*D*	diffuser
$\dot{Q}$	heat transfer rate, kW	*s*	solution or strong solution
T	temperature, K	*r*	refrigerant
h	specific enthalpy, kJ kg^{-1}	*cv*	control volume
s	specific entropy, kJ kg^{-1} K^{-1}	*IL*	ionic liquid
f	flow ratio	*w*	weak solution
GTL	gross temperature lift		
x	mass fraction of absorbent, wt%		
Greek symbols			
η	efficiency or effectiveness		
ρ	density, kg m^{-3}		
α	regression parameter for EMIM density		
β	regression parameter for EMIM density		

1 Introduction

Increasing energy demands besides decreasing the fossil fuel resources have incentivized the energy industry community to increase the efficiencies of current energy systems and utilizing alternative clean energy resources/renewables as much as possible.

There is abundant low-temperature heat coming from industrial waste or solar heat which has shown a great potential to be employed in more useful applications. The term “heat pump” refers to a thermal system that transports heat from a low temperature source into a high temperature sink [The book of Sanford Klein]. Considering the fact that within the common heat pumps, considerable amounts of energy is consumed by compressor, absorption heat pumps (AHPs) have been introduced wherein the absorption compressor including generator and absorber, has been replaced in place of common compressors. Absorption cycles can also be used to upgrade heat from renewable energies which are mostly in low-temperature levels such as solar ponds [1]. Low-grade waste heat needs to be upgraded to be used, devoid of direct heating such as residential areas or industrial buildings. By upgrading low-grade waste heat and increasing its temperature to above 100 °C, the applications increase. Absorption cycles have gained considerable attention due to their broad application area, such as waste heat recovery [2], air conditioning [3], refrigeration [4, 5] , power generation and cooling [6, 7], energy conservation [8], low-grade heat transport over longer distances [9], hydrogen generation [10], solar power utilization [11-13], improving CO_2 capture [14], desalination technologies [15, 16], and hydrogen liquefaction [6, 7].

1.1 Absorption heat transformers

Absorption heat transformers or AHTs are the second category of absorption heat pumps (AHPs) used to upgrade waste heat to higher temperature levels. AHTs are devices which deliver heat at higher temperatures than the temperature of the input heat. They have the capability to upgrade up to 50% of the low temperature/waste heat into more useful temperature levels [17, 18]. The implementation of absorption heat transformers into various thermodynamic cycles plays an important role in recovering the heat rejected by them and increasing the energy efficiency of the whole system. Absorption heat transformer is a type of absorption heat pump that operate in the opposite way of a traditional AHP (refrigeration cycles). This means that AHTs use low-grade heat to increase the output heat temperature level. AHTs are mainly categorized into single, double and triple stage absorption heat transformers (SAHTs, DAHTs, TAHTs). The SAHT basically consists of an evaporator (EV), a condenser (CO), a generator (GE), an absorber (AB), and a solution heat exchanger (SHE) (figure 1.1).

The waste heat is supplied to the generator and evaporator simultaneously and the upgraded heat is extracted from the absorber for the various applications mentioned above. The AHT cycle uses a refrigerant–absorbent solution rather than pure refrigerant of compression-based heat pumps, as the working fluid. The absorbent acts as the secondary fluid to absorb the primary fluid, which is the refrigerant in its vapour phase [17].

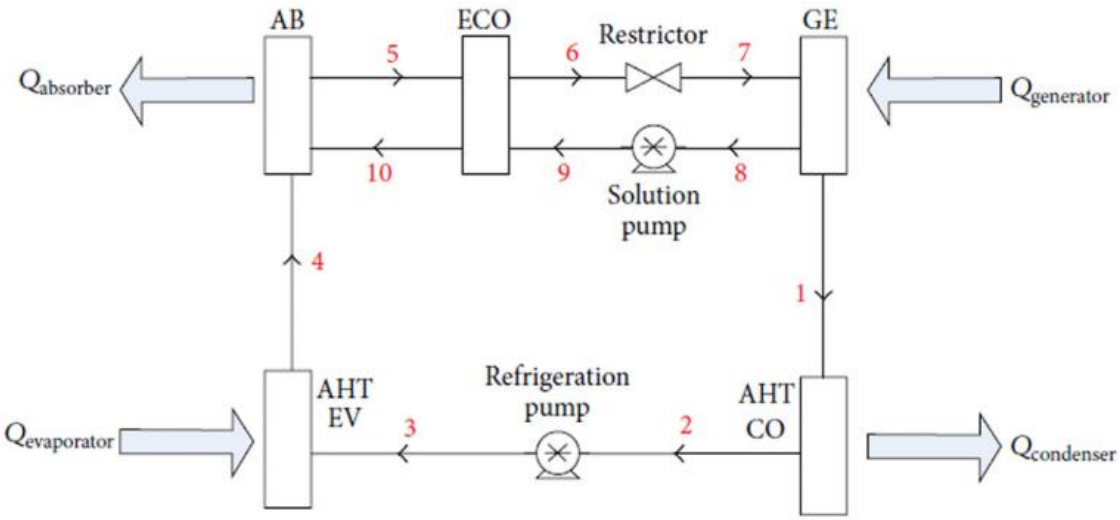

Figure 1.1 Simplified schematic of single-stage absorption heat transformer [19].

The most common working fluids used in AHT cycles are a mixture of water and lithium bromide (H_2O-LiBr) and ammonia water (NH_3- H_2O).

In generator, some amount of refrigerant vapour is removed from the weak solution and directed to the condenser. Consequently, the remaining strong solution returns to the absorber. After condensing the vaporized refrigerant in the condenser, it is pumped into a higher-pressure level as it enters the evaporator. The waste heat delivered to the evaporator provides the demanded heat of vaporization by means of low or medium-grade heat sources.

The conducted strong solution from the generator into the absorber reacts with the refrigerant vapour coming from evaporator through an exothermic reaction. Following that, the weak solution returns to the generator and the cycle is completed [19]. The released heat from the absorber is at higher temperature than the input heat in generator and evaporator due to the exothermic reaction of a working fluid such as H_2O-LiBr.

Numerous researches have been carried out on studying single-stage absorption heat transformers [19-21]. In the literature, by adding any stage to a SAHT, a temperature lift of between 30-50°C is commonly observed. So, it is possible to attain a higher temperature lift by adopting a double absorption heat transformer or a TAHT. These last two configurations deliver higher temperature lifts, but their COP decrease as a result [21].

Single stage heat transformers and two stage heat transformers can achieve gross temperature lifts (GTLs) of approximately 50 °C and 80 °C, respectively. In many industrial applications however, heat at temperatures more than 200°C may be required, a requirement which neither single stage nor two stage heat transformers are generally capable of achieving. In such situations, a TAHT can provide the demanded heat by means of mid/low level heat input which lies in the range of 50-90°C. By applying a TAHT a GTL of 140°C can be achieved [21].

In addition to the various AHT configurations, different working fluid pairs have attained a large focus in research. There have been many papers written on the comparison of different working fluid pairs. The next section will go into some detail on this topic. The focus will be mostly on SAHTs configurations, but papers using other configurations will also be investigated.

Hence, the application of AHTs can greatly aid in energy recovery and production. This energy can be utilized in a wide range of applications, such as providing clean drinking water for areas in desperate need of it, or to aid in combatting man-made contributions to climate change. Existing industries can apply AHTs to recuperate waste heat otherwise wasted, and new industries in the renewable energy sector particularly can be realized, such as examples as solar ponds and geothermal heat. For these reasons, it always in our interest to further study additions and modifications possible to the AHT cycle so that improvements can be made, and in that process access to pre-existing and new energy resources will increase.

2 Literature review

2.1 Working fluid pairs – refrigerant-absorbent: Conventional solutions

As mentioned earlier, the conventional working fluid pairs of absorption cycles are lithium bromide-water and ammonia-water. NH_3-H_2O and LiBr-H_2O have been extensively used as the working pair of absorption heat transformers in the literature [22, 23]. Stephan et al. [22] studied the thermodynamic analysis and optimization of a single-stage absorption heat transformer using ammonia-water as the working fluid. A similar study was carried out by Eisa et al. [23] investigating the thermodynamic design data for an absorption heat transformer, operating by water-lithium bromide. In the following decades, numerous papers have been published studying the absorption heat transformers using water-lithium bromide as the working fluid [2, 17, 24-32].

H_2O-LiBr is one of the most popular solutions for several reasons. Water owns a high latent heat of evaporation and is also inexpensive, nontoxic, and nonexplosive. A drawback of using water as refrigerant, is the operational temperatures used in AHTs, where the pressure levels are sub-atmospheric. LiBr interacts with water in a good manner, where it manages large internal temperature difference between heat sources and sinks which leads to a large temperature lift. In a H_2O-LiBr solution, the water is non-volatile, meaning there is no LiBr mixed with water vapour leaving the generator, and consequently, no analyser or rectifier are required within the system. On the other hand, NH_3-H_2O has some major advantages in comparison to H_2O-LiBr solution. Water as an absorbent has a very strong affinity for the ammonia vapour. In addition, both the two elements are mutually soluble over a wide range of operating conditions, and both the fluids are very stable and are compatible with most materials. This is beside the high latent heat value of ammonia refrigerant [32].

However, both the conventional working fluid pairs have their own problems. Essentially, LiBr is a salt, and therefore it has a crystalline structure. Like any other salts, depending on the temperature, it will precipitate out of the solution and will crystalize into a solid phase. This causes major issues for AHTs and generally speaking any other thermodynamic cycles using LiBr, since it will crystallize and block

the working chamber. This means that AHTs employing LiBr requires maintenance periods where the cycle needs to be shut down leading into decreasing cycle efficiency and increasing operational costs. Minimizing the crystallization risk is possible by means of employing higher temperatures through double and triple AHTs. Doing this however, will decrease the COP of the cycle [33]. Beside of crystallization problem, corrosion, high viscosity and limited solubility stand as the other issues [32]. Salehi et al. [33] investigated the crystallization risk in different types of AHTs using H_2O-LiBr. They found that at higher absorber temperatures, the pressure of the solution exiting the throttling valves dropped suddenly causing a fraction of it to be vaporized and solution concentration to be increased. This means that crystallization risk is very high next to the throttling valve, at the inlet of the generator. Additionally, they demonstrated that crystallization occurred at lower condenser and higher absorber temperatures. Another way of handling the LiBr crystallization is done by adding inhibitors or boosting the solubility using ternary solutions. But, adding chemicals increases the toxicity and corrosivity of the solution, which cause other problems [34].

The main issue regarding using ammonia as the refrigerant is the fact that water as absorbent is reasonably volatile, so the ammonia vapour leaving the generator usually contains substantial amounts of water vapour. To counter this, an analyser and a rectifier can be installed to remove the water vapour from the mixture leaving the generator before it reaches the condenser. On the other hand, higher pressures up to 50 bars and consequently higher pumping costs are demanded which makes it economically disadvantageous. The pumping costs, coupled with the need for additional equipment (analyser and rectifier), increases the cycle's complexity compared to LiBr, which increases costs. There is also the safety aspects regarding the handling of highly pressurised ammonia, which requires additional protection and prevention protocols, due to its volatility, toxicity, and flammability [32]. Comparisons between the two conventional working fluid pairs have been carried out extensively in the literature. Horuz and Kurem [32] analysed an absorption heat pump (AHP) and absorption heat transformer (AHT) using ammonia-water (NH_3-H_2O) and water-lithium bromide (H_2O-LiBr). Their study compared the coefficient of performance (COP), the flow ratio (FR) and the maximum system pressure.

It was concluded that the AHT system using water-lithium bromide solution provided better performance than the system using ammonia-water solution.

2.2 Working fluid pairs – refrigerant-absorbent: Alternative solutions

To counter the mentioned issues of conventional working fluid pairs, studies in recent decades have focused on finding alternative solutions. In the late 1980s and early 1990s studies were carried out using hydro-chloro-fluoro-carbons (HCFC) such as R21 and R22 as a working fluid in vapour AHTs [35, 36]. George and Murthy [35] ran tests on a 3 kW heating capacity R21-DMF vapour absorption heat transformer to study the influence of operating temperature on its performance. The results relied on the investigation of COPs in the range 0.2 to 0.35, exergetic efficiencies ranging from 0.3 to 0.4, and the heat delivery temperatures and temperature lifts of 85°C and 20°C, respectively. Fatouh and Murty [36] studied the different working fluid combinations of R22 as refrigerant and six absorbents including DMF, DMA, NMP, DMEDEG, DMETEG and DMETrEG in a vapour AHT. They concluded that on the overall consideration, R22-DMA and R22-NMP may be preferred for vapour AHT applications.

Ciambelli and Tufano [37] carried out a technical and economic feasibility analyses of a single-stage H_2O-H_2SO_4 heat transformer. It was proved that, the solution was particularly suited for high temperature operations, i.e. temperatures above 100°C and the lowest temperature the operation could still function at was around 80°C.

Zhuo and Machielsen [38] investigated the performance of high-temperature AHTs (single, double and triple effect) with Alkitrate as the working pair and compared with that of H_2O-LiBr. It was found that Alkitrate performed well at higher temperatures up to 260°C. However, low temperatures needed to be avoided when using Alkitrate, due to the poor solubility of the solution. Hence a working fluid with low condensing temperature, such as water would not work with Alkitrate. It performed better than H_2O-LiBr under identical operating conditions.

Water-Carrol mixtures have also been investigated in several studies [39-41] and was considered as a potential replacement for the conventional working fluid pairs [41, 42]. Carrol is a mixture of lithium bromide and ethylene glycol [$(CH_2OH)_2$] in the ratio 1:4.5 by weight. Rivera et al. [41] did a theoretical comparison of various AHT configurations with both water-lithium bromide and water-Carrol solutions. In all three configurations, at higher absorber temperatures, higher COPs and GTLs were obtained using H_2O-Carrol solution over the values obtained using H_2O-LiBr solution. The H_2O-Carrol solution also had a higher solubility and did not have the crystallization risk at lower temperatures that H_2O-LiBr solution does. It was concluded that the AHTs operating with H_2O-Carrol solution may operate over a larger range of generator and evaporator temperatures. Sotelo and Romero [42] carried out an experimental investigation on the same topic, comparing COPs between using water-Carrol mixture and water-LiBr mixture. It was found that both the GTL and COP was higher for the water-Carrol mixture compared with the water-LiBr solution.

Yin et al. [43] carried out a comparative performance study for single stage AHT using different working fluids including H_2O-LiBr, TFE-NMP, TFE-E181 and TFE-PYR. They revealed that H_2O-LiBr solution was superior to the other three mixtures when the output temperature was below 150°C, and at the temperatures higher than that H_2O-LiBr demonstrated both high corrosiveness and crystallization problems. It was therefore concluded that H_2O-LiBr was suitable at lower operating conditions, while TFE-NMP, TFE-E181 and TFE-PYR were suitable for higher operating temperatures. Other studies have also been carried out on TFE-PYR and TFE-E181 by Zhuo and Machielsen [44], and Zhao et al. [45], respectively.

2.2.1 Alternative solutions: Ternary solutions

The novel approach of using ternary or quaternary solutions rather than that of using the traditional working fluid pairs stands as a novel method of improving the performance of absorption cycles. Contrary to the common working pairs, which consist of two liquids; a refrigerant and an absorbent,

ternary solutions are comprised of three fluids, whilst quaternary solutions are encompassed of four fluids. This is done to increase the solubility of the solution. It makes it possible to gain higher concentrations of solution which is quite effective to overcome the crystallization problem. Barragan et al. [46] carried out an experiment evaluating the performance of two different ternary solutions namely water-lithium chloride-zinc chloride and water-calcium chloride-zinc chloride solutions as working pairs. By comparing GTLs, it was found that the first solution, water-lithium chloride-zinc chloride, performed better, owning a GTL of 37.5°C for an absorber temperature of 99°C. The water-lithium chloride-zinc chloride solution also exhibited lower viscosity than that of the water-calcium chloride-zinc chloride solution.

2.3 Working fluid pairs – refrigerant-absorbent: Ionic liquids

An ionic liquid (IL) is a type of salt, sharing several characteristics with those of conventional salt absorbents. In an ionic salt the ions are poorly coordinated, which leads to preserve the solvents in the liquid phase below a certain threshold temperature depending on the type of ionic liquid. The temperature range in which IL stays at liquid phase varies from several hundred degrees Celsius down to room temperature. The interest in ionic liquids as the working fluids used in absorption cycles, have gained tremendous focus within recent years [34, 47-54]. The main advantages of ILs in comparison to conventional H_2O-LiBr solutions are considered to be no crystallization risk, no high corrosion and viscosity, in addition to being non-flammable, thermally stable and having negligible vapour pressure.

Zhang and Hu [47] investigated a single-stage AHT using the ionic liquid 1-ethyl-3-methylimidazolium dimethylphosphate, and water (H_2O-[EMIM][DMP]) and compared with H_2O-LiBr and Trifluoroethanol-tetraethylenglycol dimethylether (TFE-E181) working pairs. It was proved that the new ionic liquid performed better than TFE-E181 working fluid, whilst it performed slightly worse than H_2O-LiBr solution. Although the performance of the IL was not as well as H_2O-LiBr, it did not carry the same downsides.

Zhang et al. [48] reported the results of an AHT utilizing the ionic liquid of 1,3-dimethylimidazolium dimethylphosphate ([MMIM][DMP]) and water as the working fluid pair. The simulation showed that when the condenser and generator temperature were 35°C and 90°C, with the absorption temperature not exceeding 120°C, the COP would reach 0.4 for H_2O-[MMIM][DMP], while it could reach 0.49 for H_2O-LiBr.

Ayou et al. [49] investigated the thermodynamic performance analysis of a single-stage absorption heat transformer (SAHT) and a double absorption heat transformer (DAHT) employing (1-ethyl-3-methylimidazolium tetrafluoroborate ([emim][BF4]) and 1-butyl-3-methylimidazolium tetrafluoroborate ([bmim][BF4])) as the absorbent and 2,2,2-trifluoroethanol (TFE) as the refrigerant. The performance of the ILs were compared with the performance of conventional H_2O-LiBr solution, as well as organic TFE-TEGDME solution. They revealed that for the SAHT, the COP and ECOP of TFE-[emim][BF4], TFE-[bmim][BF4] and TFE-TEGDME were lower than that of H_2O-LiBr solution at the all considered operating conditions.

Chen and Liang [54] investigated the thermodynamic performance of a single-stage absorption heat transformer using [mmim]DMP-H_2O and [mmim]DMP-CH_3OH and compared the performance with that of H_2O-LiBr. The COPs and ECOPs of the ILs performed 10% less than that of H_2O-LiBr, whilst the GTLs were higher for the ILs.

Sujatha and Venkatarathnam [52] investigated the viability of five different imidazolium based ionic liquids as the absorbent, and ammonia as the working fluid as a potential alternative of conventional solutions within a single-stage absorption heat transformer. The trend of COP values were very similar for all the five working fluids, but by comparing the ECOP quantities, it was found out that obtaining around 50% exergy efficiency with the ionic liquids of [emim][AC] and [emim][SCN] with ammonia as the refrigerant was possible. They concluded that [emim][AC] and [emim][SCN] had the potential to be utilized as the working fluid in medium temperature lift applications.

Merkel et al. [53] presented the experimental results of a single stage absorption heat transformer (AHT), using 1-ethyl-3-methyl-imidazolium methanesulfonate [EMIM][OM] and compared with those of H_2O-LiBr, H_2O-Carrol and TFE-E181. The working fluid H_2O-[EMIM][OM] showed comparable results to TFE-E181 but performed poorer in terms of COP and GTL in comparison with H_2O-LiBr and H_2O-Carrol.

Table 2.1 Summary of single-stage absorption heat transformer presented section 2.1 - 2.3

Working fluid combination (refrigerant-absorbent)	Operating conditions	Reference
NH_3-H_2O	Source temperature 90°C, sink temperature 15°C	[22]
NH_3-H_2O, H_2O-LiBr	Source temperature 70°C, condenser temperature 30°C	[32]
R21-DMF	Source temperature 70°C, condenser temperature 20-40°C	[35]
R22-DMF, DMA, DMEDEG, DMETEG and DMETrEG	Generator temperature 60°C, condenser temperature 20-50°C	[36]
H_2O-H_2SO_4	Feed temperature 80°C, condenser temperature 15°C	[37]
Alkitrate	Generator temperature 105°C, condenser temperature 50°C	[38]
H_2O-Carrol, H_2O-LiBr	Generator temperature 60-100°C, condenser temperature 20-40°C	[41]
H_2O-LiBr, TFE-NMP, TFE-E181, TFE-PYR	Generator temperature 50-70°C, condenser temperature 10-40°C	[43]
(H_2O-[EMIM][DMP], H_2O-LiBr, TFE-E181	Generator temperature 70-90°C, condenser temperature 30-40°C	[47]
H_2O-[MMIM][DMP], H_2O-LiBr	Generator temperature 90°C, condenser temperature 30-40°C	[48]
TFE-[emim][BF4], TFE-[bmim][BF4], H_2O-LiBr, TFE-TEGDME	Waste heat temperature 60-80°C, sink temperature 20-40°C	[49]
[mmim]DMP-H_2O, [mmim]DMP-CH_3OH, H_2O-LiBr	Generator temperature 70-100°C, condenser temperature 30-45°C	[54]
[hmim][Cl]-NH_3, [emim][AC]-NH_3 [emim][ETSO4]-NH_3, [emim][SCN]-NH_3 [emim][TF2N]-NH_3	Generator temperature 70°C, condenser temperature 25-35°C	[52]
H_2O-[EMIM][OM]	Heating temperature 95°C, cooling temperature 25°C	[53]

2.4 Ejector

When it comes to improving the temperature lift in an absorption heat transformer cycle, there are two primary ways of doing it. For improving the function of AHTs, lots of efforts have been carried out. Most of the studies have focused on adding more stages and complicated configurations for gaining higher GTLs. This is done by the fact that more complex configurations allow for an increase in evaporator pressure, which in turn allows for higher absorber pressure (P_{eva} = P_{abs} by neglecting pressure losses). Naturally, a higher absorber pressure allows for higher temperature lifts. Another technique for improving the temperature lift is to increase the absorbent solution concentration. This will lead to absorbing more solution, which in turn increases the GTL.

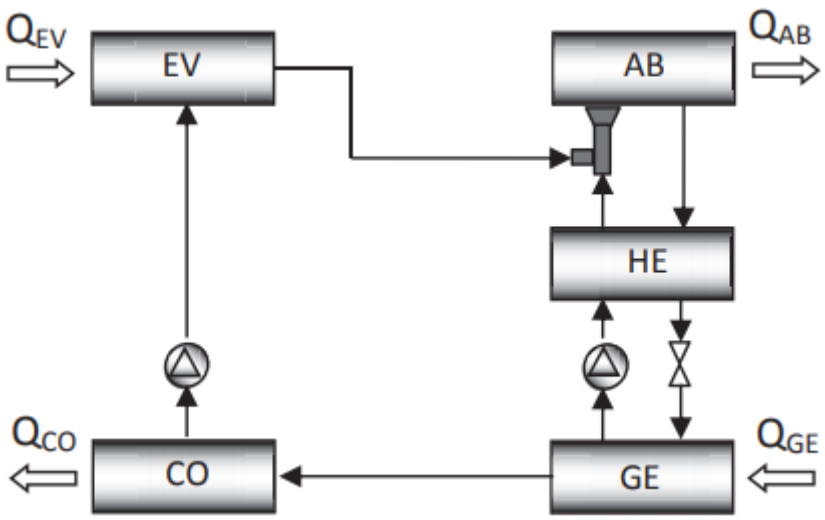

Figure 2.1 Schematic diagram of an ejector-absorption heat transformer (EAHT) [20]

The setup of ejector absorption heat transformer or EAHT is demonstrated in Figure. 2.1 where instead of generating a higher pressure in the evaporator, an ejector is mounted at the entrance of the absorber. The ejector will increase the pressure of the working fluid pair coming from the evaporator and the generator, before entering the absorber. The main advantage of applying ejector, rather than compressor, pump or blower is the fact that an ejector does not consume mechanical energy directly. Previously some works have been conducted on the application of ejectors on absorption cycles [55-57]. Most of them have focused on refrigeration cycles rather than that of AHTs [10, 13, 58-63]. Shi

et al. [55] analysed the performance of an ejection-absorption heat transformer, based on the previous performance analysis data from SAHT, DSAHT, and DAHT configurations. The study used a set of fixed values applying to the generator temperature of 70°C, condenser temperature of 30°C, and a concentration difference, Δx of 4.5%. It used five performance indicators: COP, exergy efficiency (ECOP), flow ratio (f), absorber temperature (T_{abs}) and compression ratio (ε).

$$\varepsilon = \frac{P_{abs}}{P_{eva}}$$

It was found that the EAHT performed better overall and delivered higher temperature lift to that of the SAHT.

Additionally, it was shown that ejection-absorption heat transformers were a new and promising system for recovering waste heat, with capabilities better than that of the conventional absorption heat transformer. Sözen et al. [56, 57, 64] investigated the use of ejection-absorption heat transformers in upgrading the heat provided by a solar pond. The earliest paper [56] focused on determining performance parameters using artificial neural-networks (ANNs), as a function of EAHT's working temperatures. On the second paper [57], they investigated the performance improvement of an EAHT by developing and applying a mathematical model. It found that the COP of the system improved by 14% at the maximum efficiency condition by adding an ejector. The AHT without an ejector attained the ECOP of 0.44-0.74 at evaporator and generator temperatures between 58–90°C. By adding an ejector, the ECOP of the cycle improved by 30% at the maximum efficiency condition.

The study also investigated the exergy losses of the various components, for investigating the effect of adding an ejector. The results are summarized in Table. 2.2:

Table 2.2 Summary of exergy loss in the different components [57]

Components	Non-ejector	Ejector
Absorber	90%	78%
Generator	10-20%	20-30%
Condenser	5%	Negligible
Evaporator	3%	Negligible

Since the non-dimensional exergy losses of the evaporator and condenser were so low, the values and the changes made to them by adding an ejector were negligible. They proved the feasibility of using an EAHT to increase the temperature of the heat obtained from solar ponds, beside the fact that adding an ejector to the cycle increased the performance and improved on exergy losses.

2.4.1 Ejectors: Absorption refrigeration cycles

As mentioned previously, absorption chillers have been investigated much more thoroughly on the topic of adding an ejector than that of absorption heat transformers. They are very similar, and they differ in the application of the waste heat provided to the respective systems and some minor changes on the configuration of the system. In an absorption chiller, the goal is to use the waste heat to cool down an area, for example in the application of an air conditioner. The pressure levels in an absorption chiller are much lower, which makes the temperatures attained in the absorber much lower as well. Since both the applications are so similar, knowledge can be transmitted between the two on the topic of ejector-absorption cycles. Following is a review of the literature for ejectors-based absorption refrigeration cycles.

Chen [65] investigated the addition of an ejector to an absorber cycle by the goal of improving the COP of the system. R22-DME TEG was used as the working fluid. The maximum COP for the ejector-absorber cycle found was 0.85, compared with the COP of the conventional cycle at 0.68.

Wang et al. [13] studied a solar-driven ejection-absorption refrigeration cycle and three main modifications/adding components were carried out for improving the performance of the system,

1. A three-way valve.
2. A second solution pump.
3. Adjustable reabsorption ratio of the strong solution and/or boosting of the pressure difference of the second solution pump.

Most of the values of the different COPs were found to be higher than that of the COPs of the conventional cycle.

Vereda et al. [61] conducted a study on the effect of installing an ejector with an adaptable ejector nozzle in a absorption refrigeration cycle. The purpose of the study was to evaluate the influence of the ejector geometry on the cycle performances and to determine the range of the heat source temperature in which it is convenient to use a practical ejector in the absorption cycle. The performance of the new adaptable ejection-absorption refrigeration cycle was compared with the conventional cycle, where there is no ejector installed. COP was used as the performance indicator. It was found that the diameter of the mixing tube had a great influence on the performance of the cycle.

Garoushi Farshi et al. [62] performed a thermodynamic analysis and comparison between two absorption refrigeration cycles, one with an ejector installed before the absorber, and one without. The cycle used two different working fluids, ammonia-$LiNO_3$ and ammonia-NaSCN, comparing the performance between the two. They found that using an ejector with either working fluid pair improved the performance of the cycle. Adding an ejector was found to be very efficient at lower generator temperatures. The study also investigated crystallization risk and found it to be the same regardless of the ejector. Lastly, the study investigated exergy losses in the different components and

found them to be the highest for the generator and absorber, as well as the solution heat exchanger at low generator temperatures. Finally, a sensitivity analysis was carried out to determine which variable had the greatest effect on COP and exergy efficiency, and it found that the effectiveness of the heat exchanger was the variable with the greatest effect.

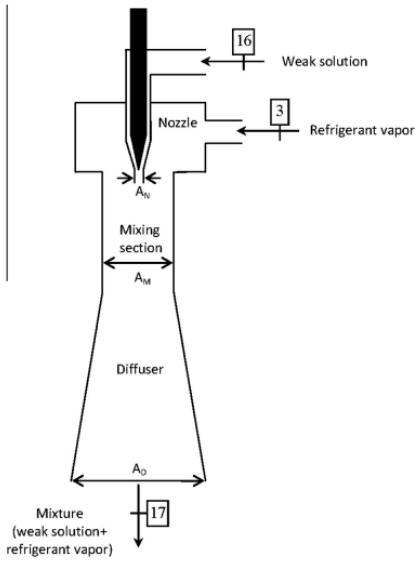

Figure 2.2 Schematic diagram of ejector used at entrance of the absorber [62]

Li et al. [63] conducted a thermodynamic analysis on a novel air-cooled non-adiabatic ejection-absorption refrigeration cycle using R290-oil mixture as the working fluid pair with the cycle being powered by exhaust gas. The study used COP and circulation ratio as the performance indicators for the simulation.

The results compared conventional absorption-refrigeration cycle with ejector absorption-refrigeration cycle, using ranges T_{eva} = -5-10°C, T_{con} = 36-47°C and T_{gen} = 76-117°C. The EARC showed better performance than that of ARC for all the working conditions. It was found that the EARC performed especially well under lower generating and evaporating temperatures. E.g. at T_{eva} = 10°C and T_{gen} = 83°C COP values of ARC and EARC increased from 0.1417 to 0.5249. Overall, the COP of the EARC under lower temperatures was overall better than for ARC, allowing for a wider working condition range for the EARC. This result was credited to the ejector, since it boosts the absorption

pressure in EARC. The EARC obtained a maximum COP of 0.5297. The study concluded that the air-cooled non-adiabatic absorber and the ejector applications are beneficial to both miniaturization and cost reduction of absorption refrigeration system, broadening the application range of the system.

2.5 AHT applications

As mentioned earlier there are lots of application for AHTs in applied industry. Waste heat or low/ mid temperature heat have very limited applications and hence AHTs can upgrade them into higher qualities. This higher quality heat has a broad range of applications previously unobtainable with low quality heat. AHTs can be installed where low-quality waste heat is produced. This section summarizes the works done in the literature on the applications of AHT cycles on more useful tasks. From manufacturing and other industrial processes to energy production, waste heat is a common bi product. By installing an AHT, the waste heat that was previously vented into the atmosphere can be captured, upgraded and utilized in the new processes and applications. This aids in raising the efficiency of energy systems and can be utilized in processes such as further products in terms of electricity production, desalination, hydrogen generation and residential heating.

2.5.1 Desalination/Water purification

Desalination is one of the most widely used application areas of AHTs [15, 16, 66-69]. Romero and Rodriguez-Martinez [66] studied a water purification systems using low-grade waste heat in an absorption heat transformer. They concluded that with the possible absorber temperatures in the range of 105-115°C, the cycle would be able to produce potable water from brackish water. For example, at T_{gen} = 80°C, T_{eva} = 60°C and T_{con} = 30°C it was possible to raise the COP_{ent} from 0.2 to 0.43 and COP_{WP} from 0.25 to 0.78 across the range of absorber temperatures. Gomri [68] studied a solar powered absorption heat transformer producing potable water from seawater from both energy and exergy points of views. Energy efficiency was found to be the highest for COP_{WP} at 0.62, and both desalination unit and flat plate collector's energy efficiency varied throughout the day, whilst AHT remained almost constant between 0.493 and 0.485.

Sekar and Saravanan [16] carried out an experimental study on a distillation system using an absorber heat transformer, where the conventional working fluid pair of H_2O-LiBr was used. COP was found to reach the maximum value of 0.38 at heat source temperature of 80°C and GTL = 15°C. The study noted that COP increased with increased heat source temperature, and at higher GTL (GTL = 20°C), the COP had a lesser value. Additionally, they concluded that the distillate flow ratio increased as a function of both heat source temperature and evaporation temperature.

Huicochea et al. [69] investigated a novel cogeneration system consisting of a proton exchange membrane fuel cell (PEMFC) coupled to an absorption heat transformer (AHT). The efficiency of cogeneration system could reach values up to 0.571, which represented an increment of around 12.4% over the fuel cell efficiency operating individually.

Parham et al. [15] carried out a comparative assessment of different absorption heat transformers for the use in desalination processes. It was proved that increasing absorber temperatures lead to decrease of COP in all configurations. The maximum amount of freshwater production for SAHT, DAHT

and TAHT were found to be 853, 796 and 697 residential units, respectively, if the systems were made to operate constantly.

2.5.2 Energy recovery/conservation

Abrahamsson and Jernqvist [70] studied the potential of incorporating an absorption heat transformer system using H_2O-NaOH as the working pair into an oleochemical plant where the waste heat was discharged to the atmosphere. The oleochemical plant produced fatty acids and refined glycerol, and in this process produces saturated water vapour at 100°C from four flash vessels used to depressurize condensate streams emerging from different processing units in the plant. The results from the economic analysis revealed that the total cost of the AHT system would be approximately 81,900 dollars, with the annual saving of steam being at 56,500 dollars. This gave a pay-off period of 1.45 years.

Currie and Pritchard [71] investigated the use of a DAHT employing H_2O-LiBr for energy recovery and plume reduction from an industrial spray drying unit. Spray drying is a method of drying which uses hot air at temperatures up to 550°C. It is widely used in the chemical industry to produce products containing only low moisture content. The recovery of heat by conventional means is not feasible, since only the sensible heat can readily be recovered, and most of the flow energy content is in the form of latent heat. Therefore, the application of an AHT can be used to recover large parts of latent heat from exhaust air streams. The study used a two-stage AHT with H_2O-LiBr as the working fluid pair.

The study found that the reduction of the visible plume could itself justify the heat transformer installation as a retrofit. By installing the AHT, fuel savings equivalent to 0.37 MW worth circa 20,000 GBP (in 1994) would be the result.

Ma et al. [2] studied the application of an absorption heat transformer to recover the waste heat from the synthetic rubber plant of Yanshan Petrochemical Corporation, Beijing, China. The study was carried out experimentally operating on a single stage AHT using H_2O-LiBr solution supplied with heat flow of

5000 kW. The AHT recovered waste heat at 98°C from a mixture of steam and organic vapour from the synthetic rubber plant. Through the economic analysis it was found that by employing AHT system, the steam consumption per ton of rubber was reduced from 2.53 ton to 1.04 ton. The payback period was calculated to be just over 2 years. The environmental benefit of using the AHT system was also remarked on, equating the 5000-kW capacity of the AHT installation to 38,200 tons of steam per year.

Yang et al. [72] carried out an investigation into using low grade heat in a novel cascade absorption heat transformer (NCAHT) for the application of producing low-pressure steam. The cascade system consisted of two subsystems operating at two different pressure levels. The high-pressure subsystem used NH_3-H_2O as the working solution, while the low-pressure subsystem used H_2O-LiBr.

The low-grade heat was divided into two parts called HTP and LTP. The HTP was used as the heat source for the H_2O-LiBr AHT, while the LTP was used as the heat source for the NH_3-H_2O AHT. High temperature heat produced by the NH_3-H_2O AHT cycle was fed into the H_2O-LiBr AHT cycle, which subsequently produced low temperature heat which was fed back into the NH_3-H_2O AHT cycle. This heat integration improved the energy utilization of NCAHT, and resulted in GTL of up to 80°C. The study concluded that the NCAHT is a promising option for energy recovery, and that the new process is both economical and saves energy.

In a subsequent study by Yang et al. [73], the same NCAHT system was applied to a coal to synthetic natural gas plant. The economic analysis takes both product price and cooling water price fluctuations and inflation into account, which showed that NCAHT were able to adapt to changes in prices. The analysis calculated a capital investment of 924,000 USD for a 12 MW NCAHT. The Financial Internal Rate of Return (FIRR) equalled 62.16% and the payback period was calculated to be 0.77 years.

2.5.3 CO2 capture improvement

Wang et al. [14] applied a DAHT for post combustion CO_2 capture in a 350 MW supercritical unit of a coal-fired power plant. By upgrading the low-grade steam in the DAHT to match the regeneration temperature in the CO_2 capture unit, it was possible to improve the performance of the system. Normally, the energy needed for regeneration is provided by steam extracted from the intermediate pressure (IP) cylinder of the steam turbine. The temperature here is commonly over 200°C, which is much higher than the desorption temperature of the rich solvent (usually between 115 to 120°C). This large temperature differential between the steam extracted and the solvent, leads to a huge exergy destruction in the CO_2 regeneration process. The upgraded heat from the DAHT makes it possible to avoid extracting this high-level steam from the IP cylinder. This will reduce the exergy destruction of the regeneration process, which will result in a higher exergy efficiency.

At the optimum CO_2 capture rate, the proposed system could save 28.07% in energy consumption compared to the reference system. The energy level difference between energy donor (steam extracted) and the recipient (solvent) was found to be reduced by 90%. The exergy destruction in the CO_2 separation and steam condensation process was therefore 49.5% lower than the reference system. Finally, the findings from the economic analysis found that with 53.65% CO_2 capture rate, the cost of CO_2 avoided (COA) and cost of electricity (COE) could be reduced by 10.7 dollars per ton CO_2 and 1.9 dollars per MWh, respectively. The study concluded that the new CO_2 capture approach had superior thermal performances and economic benefits that made it promising for real world implementation.

3 Purpose of the study

This thesis aims to modify a simple single-stage absorption heat transformer by adding an ejector. The injector is considered at the inlet of the absorber, where the flow from the evaporator and generator combine and mix before being sent into the absorber. The goal of this modification is to study the effects of the addition of an ejector in a SAHT, investigating for two cases with different working fluids. The working fluids that will be investigated in this paper are the conventional H_2O-LiBr solution, and the novel ionic liquid of H_2O-[EMIM][DMP]. Waste heat is assumed to be provided to the generator and evaporator of the system, by the goal of using the new ejection-absorption heat transformer to upgrade the heat to higher temperatures.

At the present work the conventional working pair of H_2O-LiBr and a novel ionic liquid-water working pair named H_2O-[EMIM][DMP] have been employed in a single AHT system. Based on the authors knowledge, no previous study has been carried out investigating an EAHT using an ionic liquid. Since LiBr is a salt, using it as an absorbent has issues mainly connected to crystallization. LiBr also has other disadvantages in terms of corrosion, high viscosity, limited solubility, and a practical upper temperature limit. Therefore, interest in finding new working fluids have been done, with many studies in recent time focusing on ionic liquids. This study will look at performance of using H_2O-[EMIM][DMP] in an ejector absorption heat transformer.

The mathematical model of the ejector is based on previous work done by Garoushi Farshi et al. [62], while the overall system used and thermodynamic analysis of the complete cycle is based on work done by Kamali et al. [34]. The whole system is modelled and simulated in Engineering Equation Solver (EES). Internal functions in EES will be used for H_2O-LiBr, and a provided EES code developed by Kamali is used for H_2O-[EMIM][DMP]. The addition of ejector section to the provided code in EES is carried out by the author. The results from the simulation are validated by the available data from literature. The results will be compared against the AHT without the ejector installed, by the goal of highlighting the improvements made the performance of the new system. An energy analysis is also presented. It

is expected that the addition of ejector improves the performance of the system, which will be indicated by the performance indicators used in the study. The performance indicators are plotted in graphs and displayed in tables for easy comparison between AHT and EAHT.

4 Methodology

4.1 Systems description

The study focuses on an ejector based single-stage absorption heat transformer employing LiBr-H_2O and [EMIM][DMP]-H_2O as the working fluid. Both the configurations are illustrated in figures 4.2 and 4.3. The cycle operates at two pressure levels that are characterized based on saturation pressure of the refrigerant after condenser and evaporator (illustrated as a PT-diagram in figure 4.1).

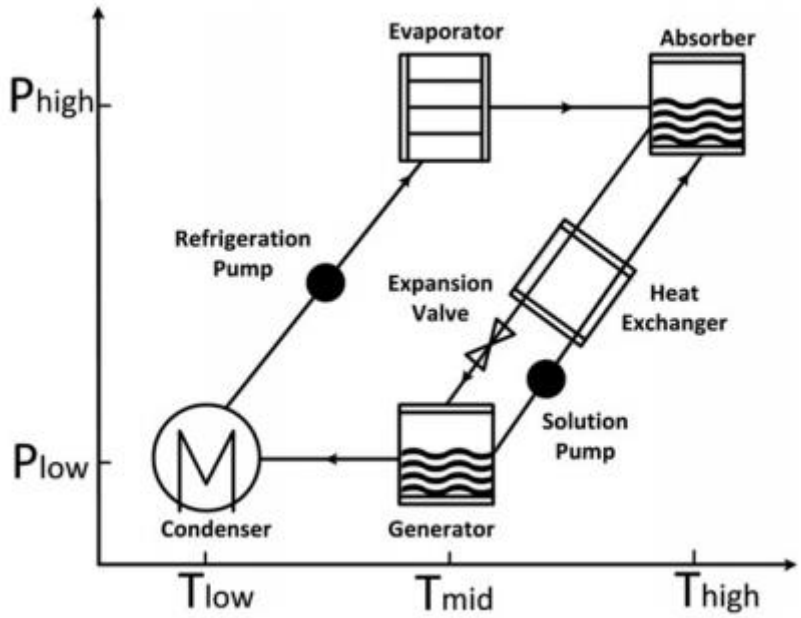

Figure 4.1 Pressure-temperature diagram of the first system [34]

The scenario of the cycle operations is as follows: Two streams, one from the generator and one from the evaporator is combined in the absorber. The stream coming from the generator contains a strong solution (high concentration of absorbent), and as the name implies it meets the refrigerant coming from the evaporator stream wherein the absorbent absorbs the refrigerant, weakening the solution. The weak solution leaves the absorber and enters the heat exchanger. The heat exchanger transfers the heat from the weak solution side to the strong solution side coming from the generator. Following the heat exchanger, the weak solution is throttled through an expansion valve, which lowers the pressure and temperature of the flow before entering the generator. By lowering the pressure and

temperature, the absorbent would not be able to absorb the refrigerant to the same extent, and large parts of the refrigerant and absorbent would separate and flow in different directions from the generator. The refrigerant continues towards the condenser, driven by the heat supplied to the generator. The same heat is also supplied to the evaporator. The absorbent travels back towards the absorber. The refrigerant is first condensed in the condenser, before it pumped towards the evaporator. This aids to increase the pressure of the refrigerant before entering the evaporator. Once more, in the evaporator the refrigerant gains the external supplied heat, the refrigerant is evaporated into saturated vapour phase. The absorbent coming from the generator is also pumped through a pump and going through the heat exchanger it is heated up before it enters the absorber together with the flow from the evaporator. In the absorber the heat is upgraded through an exothermic reaction between the absorber and refrigerant. So, the temperature in the absorber is higher than the temperature in the generator and evaporator.

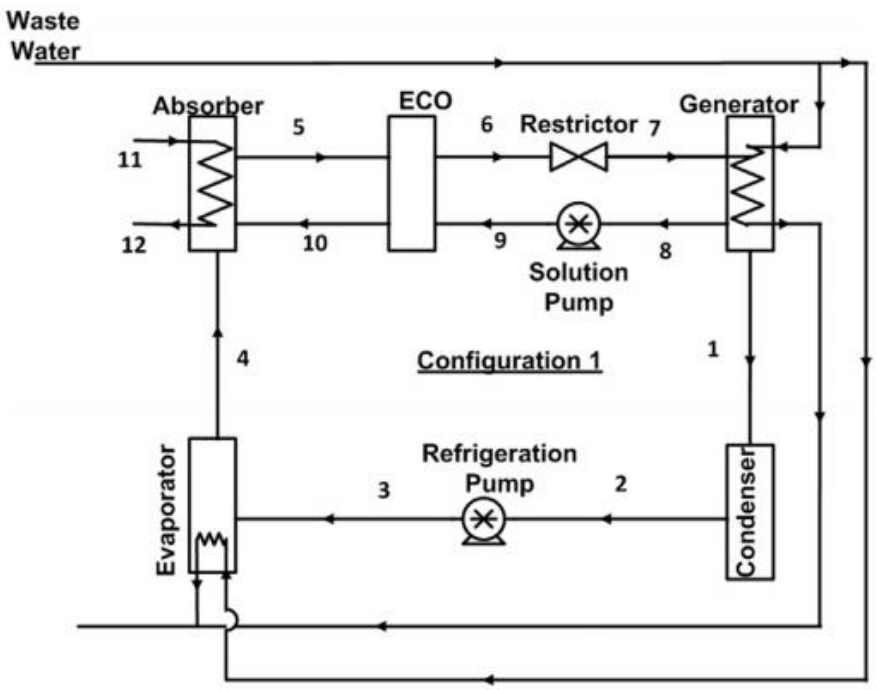

Figure 4.2 Schematic diagram of SAHT (S-Type I) [19]

By adding an ejector to the system, the stream coming from the evaporator and the strong solution coming to the generator will enter the ejector which is set in before the inflow of the absorber (figure 4.3) and the streams will be further mixed before entering the absorber. In addition, the ejector will be able to increase the pressure of the refrigerant without consuming mechanical energy directly. This means that the absorber pressure can be increased, which in turn can yield higher absorber temperature. Hence, by installing an ejector, it is possible to increase the overall performance of the cycle. For modelling the cycle, several simplifying assumptions need to be made. The considered assumptions are as follows:

1. Steady-state flow condition.
2. Kinetic and potential energy changes are negligible.
3. No pressure loss inside the respective components of the cycle.
4. Considering some efficiencies for ejector and heat exchangers. This is done to account for irreversibilities and losses to the environment.
5. The refrigerant is at saturated phases at the outlet of the evaporator and condenser.
6. The generator and evaporator are heated by the same source ($T_{gen} = T_{eva}$).
7. The mechanical work of the pump is small enough to be negligible.
8. The condenser rejects the heat to the environment.

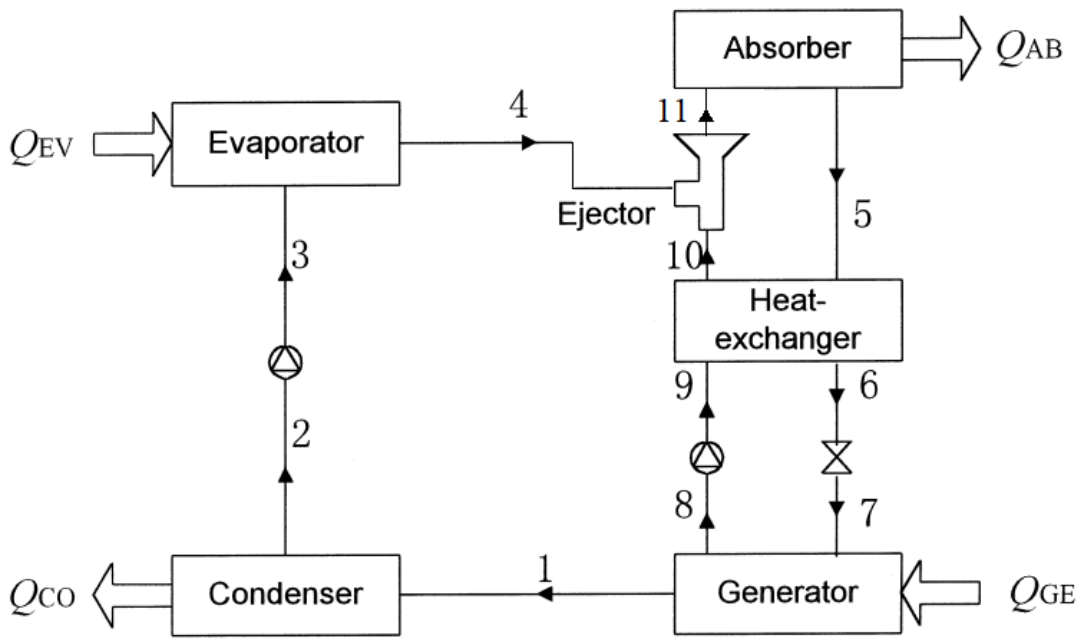

Figure 4.3 Schematic diagram of ejection-absorption heat transformer (edited by author) [19].

4.2 Thermodynamic analysis of the ejector

Adding the ejector to the AHT system greatly affect the performance of the overall system. The basis of the thermodynamic analysis of the ejector besides governing equations and assumptions are gathered from the study done by Garoushi Farshi et al [62]. The ejector simulation has been modelled based on a one-dimensional flow model. This model uses a mixing efficiency which accounts for the mixing irreversibility. The assumptions made for modelling ejector are as follows:

1. No external heat transfer occurs.
2. Primary and secondary fluids have stagnation conditions at the entrance of the ejector.
3. The weak solution flows through the nozzle from the generator pressure to the evaporator pressure.
4. The given efficiencies are to account for non-ideal conditions, e.g. friction and mixing losses.

5. All fluid properties are uniform over the cross-section after the complete mixing at the exit of the mixing section.
6. Potential energy is negligible.
7. The flow is incompressible, due to the low Mach numbers involved.
8. Absorption processes do not occur in the mixing tube and the diffuser.

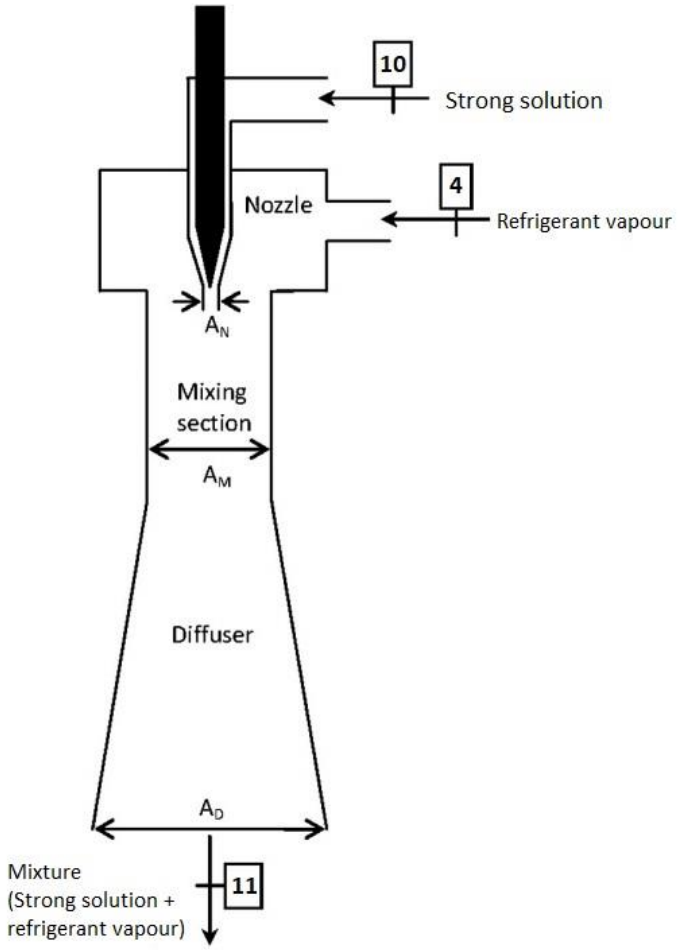

Figure 4.4 Schematic diagram of ejector used at entrance of the absorber (edited by the author) [62].

The governing equations are as follows:

Nozzle:

$$V_N = \left(\eta_N * 2 * \frac{1000(P_{con} - P_{eva})}{\rho_{10}}\right)^{0.5}$$

$$A_N = \pi * \frac{D_N^2}{4}$$

$$\rho_{10} = f(T_{10}, X_{10})$$

$$A_N = \frac{\dot{m}_9}{\rho_{10} * V_N}$$

η_N is assumed to be 0.85.

Mixing section:

$$V_M = \frac{\dot{m}_2 + \dot{m}_9}{A_M * \rho_M}$$

$$A_M = \pi * \frac{D_M^2}{4}$$

$$\rho_M = \frac{\dot{m}_2 + \dot{m}_9}{\frac{\dot{m}_2}{\rho_4} + \frac{\dot{m}_9}{\rho_{10}}}$$

$$P_M = P_{eva} + \eta_M * \frac{\dot{m}_9 * V_N - (\dot{m}_9 + \dot{m}_2) * V_M}{A_M * 1000}$$

η_M is assumed to be 0.9.

Diffuser:

$$P_D = P_M + \frac{0.5 * \rho_M * (V_M^2 - V_D^2) * \eta_D}{1000}$$

$$P_{abs} = P_D$$

$$V_D = \frac{(\dot{m}_9 + \dot{m}_2)}{\rho_M * A_D}$$

$$A_D = \pi * \frac{D_D^2}{4}$$

$$\dot{m}_9 * h_{10} + \dot{m}_4 * h_4 = \dot{m}_9 * h_{11s} + \dot{m}_4 * h_{11r}$$

$$h_{11s} = f(T_{11}, X_9)$$

$$h_{11r} = f(T_{11}, P_{abs})$$

η_D is assumed to be 0.8.

The numbers in the governing equations above are done in accordance with figure 4.3 and 4.4. The diameter of the ejector nozzle is calculated from the two formulas for A_N in the nozzle section. The diameter of the mixing section and diffuser are assumed and given a value. In this case, the mixing section diameter is set to 0.06 m and the diffuser diameter is set to 0.15 m.

4.3 Thermodynamic analyses of the systems

Mass and energy balances have been employed to both the setups. A code has been developed in Engineering Equation Solver (EES) and all the corresponding equations are considered.

The general mass balance equation can be written as,

$$\sum(\dot{m})_{in} - \sum(\dot{m})_{out} = 0$$

For each component, the first law of thermodynamics is given by,

$$\sum(\dot{m} * h)_{in} - \sum(\dot{m} * h)_{out} + \dot{Q}_{cv} - \dot{W}_{cv} = 0$$

Where $\dot{Q}_{cv}$ and $\dot{W}_{cv}$ stands for the heat flow of the component and the workflow, respectively.

The following are the energy balances for each component in the cycle (figure 4.3).

Generator:

$$Q_{gen} = m_8 h_8 + m_1 h_1 - m_7 h_7$$

Condenser:

$$Q_{con} = m_1(h_1 - h_2)$$

Evaporator:

$$Q_{eva} = m_3(h_4 - h_3)$$

Absorber for AHT:

$$Q_{abs} = m_4 h_4 + m_{10} h_{10} - m_5 h_5$$

Absorber for EAHT:

$$Q_{abs} = m_{11}(h_{11} - h_5)$$

Heat exchanger:

$$m_5(h_5 - h_6) = m_9(h_{10} - h_9)$$

$$\varepsilon_{eco} = \frac{T_{10} - T_9}{T_5 - T_9}$$

4.3.1 Performance indicators

Some important performance parameters are used to compare the performances of the two different working fluid pairs, H_2O-LiBr and H_2O-[EMIM][DMP], as well comparing the cycle with a without an ejector. The current study continues the previous work done by Kamali et al. [34], and will use the same performance indicators.

The coefficient of performance (COP) is defined as the ratio of available useful heat output of the system ($\dot{Q}_{abs}$) to the driving external heat inputs of the system (evaporator and generator heat inputs, $\dot{Q}_{eva}$ and $\dot{Q}_{gen}$, respectively),

$$COP = \frac{\dot{Q}_{abs}}{\dot{Q}_{eva} + \dot{Q}_{gen}}$$

The exergetic efficiency (ECOP) is based on the second law of thermodynamics and is defined as the ratio of the energy output of the absorber to the total available energy input of the system,

$$ECOP = \frac{\dot{Q}_{abs}(1 - \frac{T_0}{T_{abs}})}{\dot{Q}_{eva}\left(1 - \frac{T_0}{T_{eva}}\right) + \dot{Q}_{gen}(1 - \frac{T_0}{T_{gen}})}$$

where T_0, T_{abs}, T_{eva}, T_{gen} are the environmental reference, the absorber, the evaporator and the generator temperatures, respectively. Exergy itself is a thermodynamic concept, very often applied as a performance indicator to look at how well a system or components of a system perform. It is defined as "*The maximum useful work which can be extracted from a system as it reversibly comes into equilibrium with its environment*". In other words, it is the capacity of energy to do physical work.

Gross temperature lift (GTL) is the difference between the absorber and evaporator temperatures,

$$GTL = \Delta T = T_{abs} - T_{eva}$$

In fact, GTL shows the temperature lift possible using a given working fluid in an AHT. The higher the GTL is, the more capable the system is in upgrading lower quality heat to more useful heat. It is evident that at higher temperatures more useful applications such as such as desalination, hydrogen generation and electricity production are achievable while at lower temperatures only limited applications as direct heating are possible.

The concentration of the weak and strong solution is also a useful performance parameter. The strong solution is denoted as X_s and the weak solution as X_w.

$$\Delta X = X_s - X_w$$

Increasing concentration difference results in more driving force caused by mass transfer through both absorber and generator.

The flow ratio, f, is the ratio of the mass flow rate of the strong solution, in absorbent, through the solution pump per unit mass of refrigerant vapour generated by the generator,

$$f = \frac{\dot{m}_s}{\dot{m}_r} = \frac{\dot{m}_8}{\dot{m}_1} = \frac{X_7}{X_8 - X_7}$$

Flow ratio is used as a performance indicator for the cost of a given system. High flow ratio results in the need for larger equipment, increasing the capital cost of AHT cycle. Lower flow ratios are therefore usually more appreciated than higher ones when comparing working fluids.

4.3.2 Simulation basis

The calculations are done using EES software and uses the property library for H_2O-LiBr solution. For the ionic liquid on the other hand, a code developed by Kamali et al. [34] has been provided and employed for calculating the properties of H_2O-[EMIM][DMP]. The code has been modified to consider the addition of an ejector by the author. In addition, a method for calculating [EMIM][DMP] density has been added to the code.

4.3.3 Thermodynamic properties

The property library of EES has been used for H_2O-LiBr solution. Since such a property library does not exist for H_2O-[EMIM][DMP], a code has been developed to calculate thermodynamic properties. The ejector code of EES is derived from governing equations of the ejector from the literature [62], states that density for state 10 as a function of temperature and mass concentration of absorbent in solution:

$$\rho_{10} = f(T_{10}, X_{10})$$

Since density is a thermodynamic property and is not defined for [EMIM][DMP] in EES, a new method was demanded to be developed for finding the density of [EMIM][DMP] as a function of temperature and mass concentration of absorbent in solution. Gong et al. [74] reported the viscosity and density measurements of two ionic liquids in combination with water and methanol. One of the employed ionic liquids was [EMIM][DMP]. They used density measurements to create empirical correlations for calculating density of [EMIM][DMP]. It was found that from the viewpoint of the linear variation with temperature and complex variation by IL content of the density for a binary mixture, the experimental data could be correlated with by following equations:

$$\rho = \alpha + \beta * T$$

$$\alpha = \sum_{i=1}^{5} a_i x_{IL}^{i-1}$$

$$\beta = \sum_{i=1}^{5} b_i x_{IL}^{i-1}$$

Where ρ is the density in g m^{-3}, T is the absolute temperature in K, a_i and b_i are the regression parameters, and x_{IL} is the mole fraction of [EMIM][DMP]. The regression parameters are listed in table 2.1. Here T is the temperature at state 10, whilst x_{IL} represents the mass concentration of [EMIM][DMP] at state 10.

Table 4.1 Regression parameters used in density equation

i	**1**	**2**	**3**	**4**	**5**
a	1.1107	2.7534	-8.0114	9.3644	-3.7976
b	$-3.7941*10^{-4}$	$-3.6928*10^{-3}$	$1.2141*10^{-2}$	$-1.5011*10^{-2}$	$6.2714*10^{-3}$

4.3.4 EMIM density confirmation

A major challenge for the ejector code in the current work, is the method for density at stage 10 that is to be calculated. For the conventional working fluids, e.g. LiBr or $LiNO_3$ it is possible to use the in-built functions of EES to calculate the density using two independent variables. [EMIM][DMP] has no such in-built function and a code was therefore developed by Kamali et. al [34] for this purpose. The code did not include a method for calculating density. So, the code needed some modifications. A code for calculating [EMIM][DMP] density has been developed using a the equations presented by Gong et al. [74]. To confirm the results of the code, a plot (figure 4.5) was made using data from the latter mentioned work together with the results from running the code. As the graph shows, the results obtained are in satisfactory agreement with experimental data from Gong et al [74]. The decreasing linear trend of density as a function of temperature is demonstrated for all three of the results.

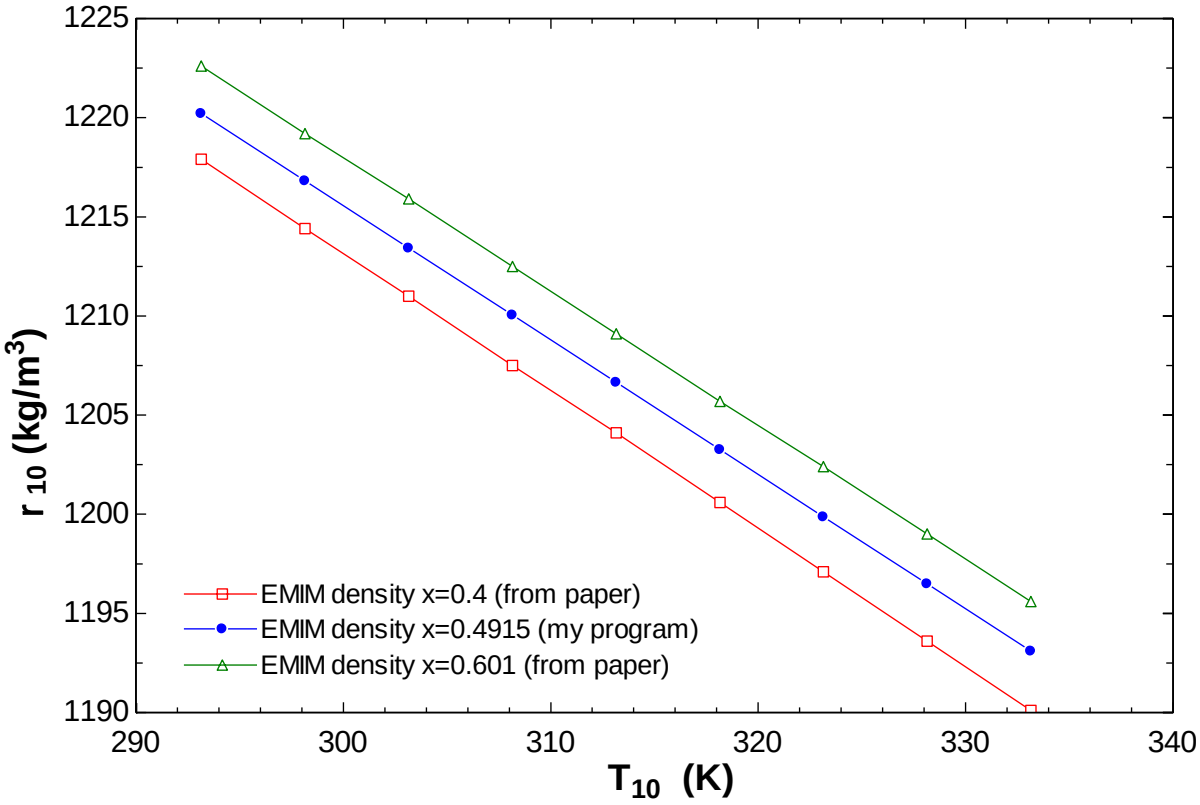

Figure 4.5 Confirmation of EMIM density calculation working as intended plotted against experimental results from Gong et al. [74].

4.4 Model validation

For the purposes of validating the obtained results of the simulation, data from Shi et al. [55] and Zhang and Hu [47] have been compared against the performance data of EAHT using H_2O-LiBr and H_2O-[EMIM][DMP] as working fluid pairs, respectively. The conditions compared against are at the same input temperatures and temperature range for both cases. Figure 4.6 compares the results of COP, ECOP and flow ratio as a function of absorber temperature from Shi et al. [55] and the present study. It is important to note that Shi et al. [55] uses a compression ratio (ratio ($\varepsilon=P_{abs}/P_{eva}$) which affects the results and alters the values of COP, ECOP and flow ratio. There are also a high likelihood that the input parameters on ejector and other parts of the system (e.g. refrigerant mass flow rate) differ in values between present study and the study of Shi et al. [55]. It is evident from figure 4.6 that the general behaviour of COP, ECOP and flow ratio are in agreement. The results can be further validated for the present study at higher absorber temperatures, where the results and behaviour are even closer to those of Shi et al. [55]. It is demonstrated in figure 4.7.

Comparing the present work and the reference study show that COP is very similar and behaves in the same manner. However, the COP decreases at a faster rate for the reference study after 105°C. COP is almost constant at lower absorber temperatures and starts to decrease at a sharper rate as the temperature increases. ECOP for reference study is higher than that of the present work, and it not only stagnates, but decreases at high temperatures. However, the behaviour correlates well, increasing across most of the temperature range. Flow ratio is higher for reference study, but both results display a rapid increase in flow ratio as temperature increases. Figure 4.7 shows a better match in values found particularly for ECOP and flow ratio. The behaviour is even closer to reference study at this temperature range. Similar behaviour of COP and ECOP of EAHT using H_2O-LiBr solution are reported by Sözen and Yücesu [57].

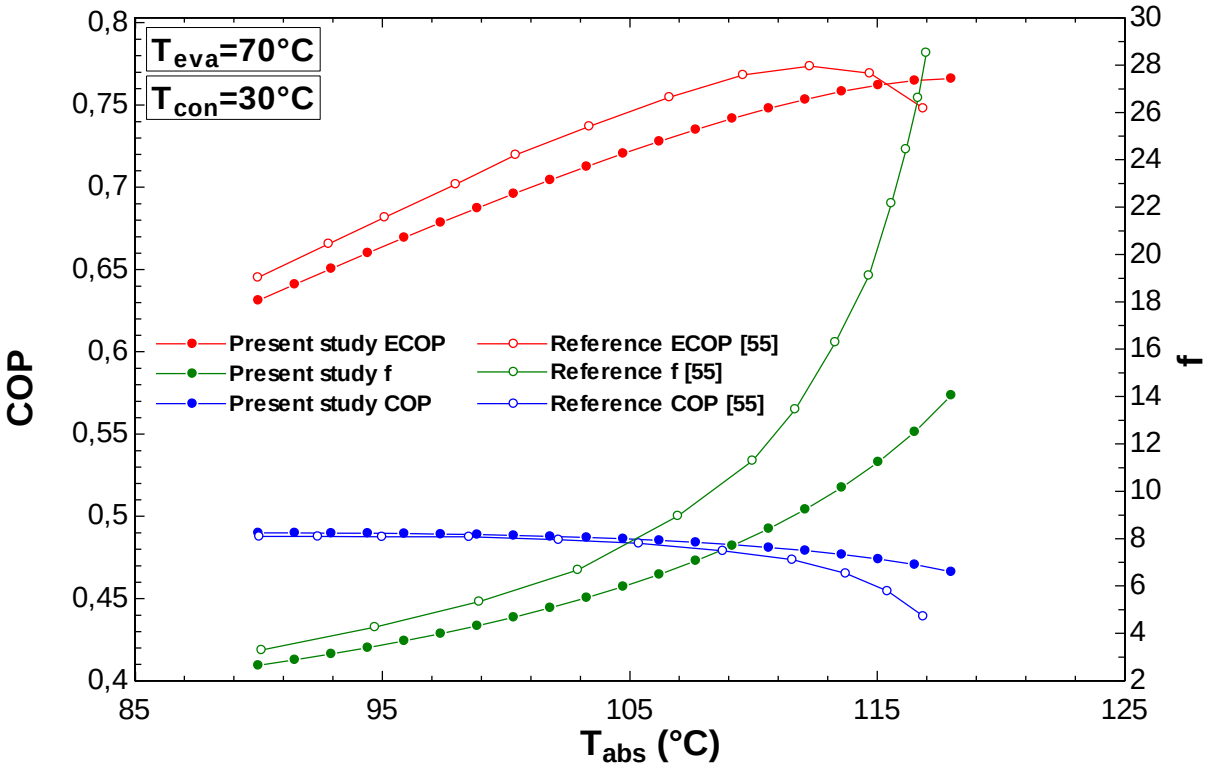

Figure 4.6 Validation of the developed simulation model using H_2O-LiBr as working fluid pair (system 1) [55]

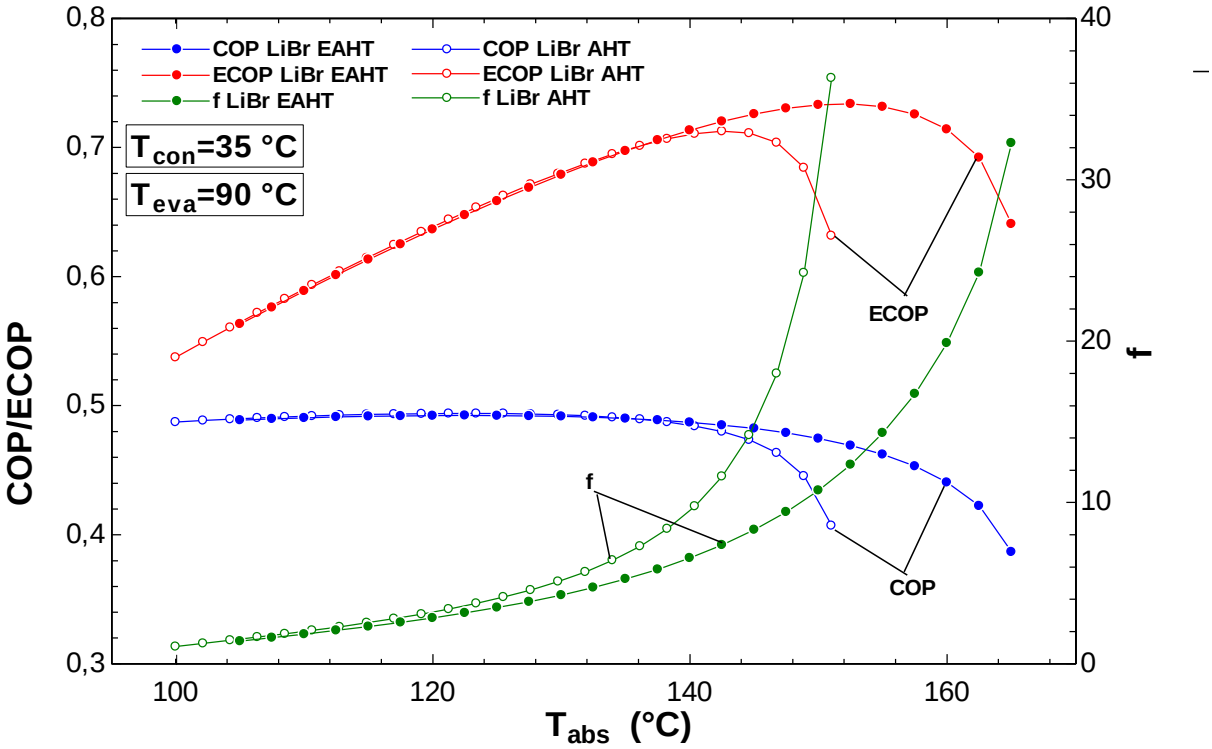

Figure 4.7 COP, ECOP and flow ratio as function of T_{abs}. For comparison to the values displayed for COP, ECOP and flow ratio of Shi et al. [55]. The values and behaviour of the three performance parameters are in good agreement here. Note the differing T_{abs} range.

Figure 4.8 is based on the work of Kamali et al [34]. It is worth mentioning that there is not any information from the literature pertaining to the topic of ejector based AHT using H_2O-[EMIM][DMP] as the working fluid. For this reason, the model has been validated by comparing it with the performance of system with no ejector. Figure 4.8 show the effect of absorber temperature on exergetic efficiency (ECOP). Once more there is a good agreement in ECOP behaviour between the results from present study, Kamali et al. [34] and Zhang and Hu [47].

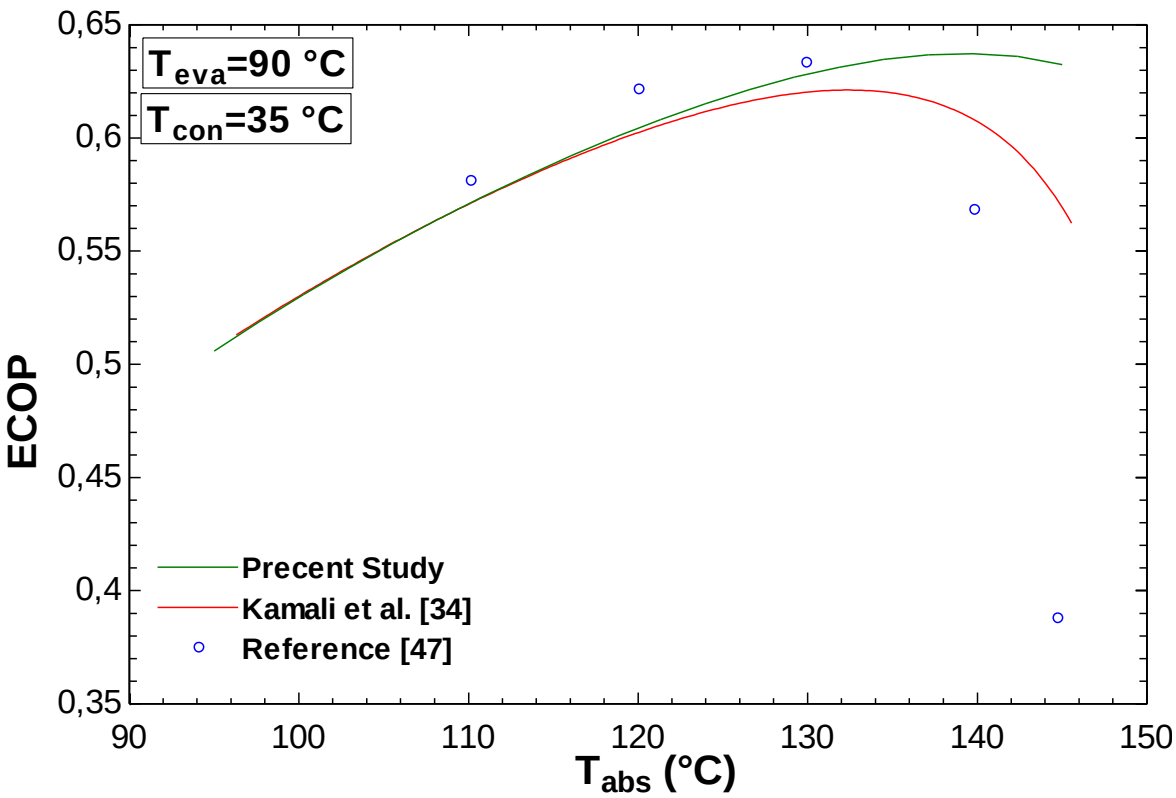

Figure 4.8 Validation of the developed simulation model using H_2O-[EMIM][DMP] as working fluid pair (system 2) [34, 47]

5 Results and discussion

Table 5.1 The input parameters of the simulation

Parameters	Unit	Value
Absorber temperature, T_{abs}	(°C)	105-155
Heat source temperature, $T_{eva} = T_{gen}$	(°C)	75-100
Condenser temperature, T_{con}	(°C)	25-40
Heat exchanger effectiveness, ε_{eco}	(%)	80
Refrigerant flow rate	(kg/s)	1
Standard temperature, T_0	(°C)	15
Nozzle efficiency, η_n	(%)	85
Mixing section efficiency, η_m	(%)	90
Diffuser efficiency, η_d	(%)	80
Mixing section diameter, D_m	(m)	0.06
Diffuser diameter, D_d	(m)	0.15

The input parameters of Table 5.1 have been used to carry out the calculations of several performance parameters. The effect of adding ejector have been investigated and compared against the AHT cycle without ejector using performance parameters such as COP, ECOP, flow ratio and solution concentration difference. The study has strictly carried out first law thermodynamic analyses and comparisons of both system 1 H_2O-LiBr and system 2 H_2O-[EMIM][DMP] with and without ejector. Table 5.2 displays the results where set input temperatures were used to calculate flow ratio, COP, ECOP, weak and strong solution concentration and the different heat outputs of the components of the system. The table displays the results of both system 1 and system 2. A higher input absorber temperature was considered for in table 5.2 and 5.3, due to the improved performance of the system regarding COP and ECOP at higher temperatures. This behaviour can be seen in Figure 5.2-5.5. Table 5.3 summarizes the calculated thermodynamic properties of AHT and EAHT, giving an overview of how the performance parameters and thermodynamic properties are affected by the addition of an absorber at set values of input temperatures.

Figure 5.1 (a)-(d) serve several purposes. Firstly, COP and ECOP values are compared as functions of generator temperature for H_2O-LiBr and H_2O-[EMIM][DMP] cycles. Here, the comparison is between both systems with and without ejector. This function for both comparing the performance of the two

systems, as well as comparing the cases with ejector with no ejector. All the 4 graphs are based on different absorber and condenser input temperature combinations. The addition of an ejector does not affect in the performance of the two systems. That is, using LiBr as the absorbent still gives a superior performance compared to the performance of [EMIM][DMP] as the absorbent. The much more interesting discovery lies in the comparisons of the respective systems with and without ejector. As can be seen in figure 5.1, the COP declines sharply for AHT of both systems at lower generator temperatures. This decline is much more linear for EAHT. At lower generator temperatures, EAHT performs better than AHT. This is particularly apparent in Figure 5.1 (b), where the absorber temperature is 130°C and condenser temperature 35°C. Here the difference of COP and ECOP between EAHT and AHT is the highest. For LiBr at 80°C there is a 58.65% increase in COP, whilst for [EMIM][DMP] at 78.5°C there is a 96.03% increase in COP. The difference quickly converges to the point almost identical performance. In fact, for LiBr at 100°C there is a 0.32% decrease in COP. On the other hand, for [EMIM][DMP] there is a 0.24% increase in COP at 100°C.

The lower the generator temperatures are, the higher the difference become. As generator temperature increases the difference shrinks, eventually converging to approximately the same values at high generator temperatures. When absorber temperature is 130°C and condenser temperature 35°C, the convergence occurs at the higher generator temperatures than for the other input temperatures. System 2 is found to converge at higher temperatures than that of system 1 for all 4 cases. The maximum value of COP as a function of generator temperature is not increased as a result of adding the ejector.

ECOP for AHT increases at lower generator temperatures, before starting a linear decline. With exception of figure 5.1 (b), this development is not seen in ECOP for EAHT. Here, the ECOP is at its maximum value at the lowest temperature and steadily decreases in a linear fashion. Similar to COP, the ECOP values converge with each other for EAHT and AHT. ECOP remains higher for EAHT than that of AHT at lower generator temperatures. As ECOP converges between the two cases it closely follows

the behaviour of COP. Maximum quantity of ECOP is found at lower generator temperatures, often as low as possible. The maximum value of ECOP is therefore increased as a result of adding the ejector. E.g. from figure 5.1 (b) the maximum ECOP of system 1 is increased by 3.81%, and system 2 is increased by 6.49%.

As demonstrated on figure 5.1 (a)-(d), it is safe to conclude that the addition of an ejector allows a much more effective utilization of lower-grade heat being supplied to a system. EAHT also starts operating at lower generator temperatures, and consequently can utilize lower temperature heat sources (e.g. solar ponds, geothermal heat). This means that EAHT have a broader application range and can be installed in industries or other areas where the heat source is too low for a traditional single effect AHT. The threshold temperature that gives significant COP and ECOP improvement varies depending on the desired GTL and condenser temperature available. E.g. for figure 5.1 (b) system 1 will benefit from an ejector addition when generator temperatures are lower than 85°C, whilst system 2 at generator temperatures lower than 95°C. Thus, system 2 has a broader temperature range in which ejector addition improves the performance of the system compared to system 1. In other words, system 2 benefits more from the addition of an ejector than system 1. Operating at lower generator temperatures also lowers crystallization risk in the case of system 1.

a)

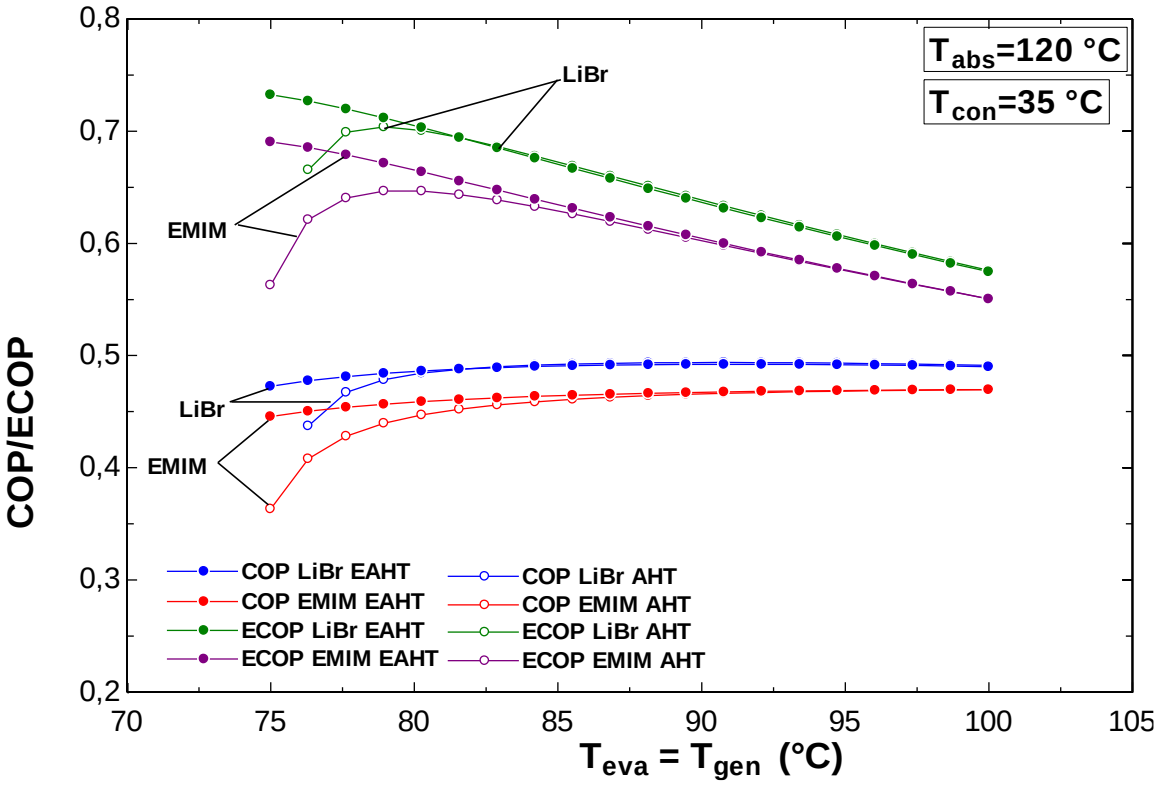
T_{abs}=120 °C
T_{con}=35 °C
LiBr
EMIM
LiBr
EMIM
COP/ECOP
T_{eva} = T_{gen} (°C)
COP LiBr EAHT
COP EMIM EAHT
ECOP LiBr EAHT
ECOP EMIM EAHT
COP LiBr AHT
COP EMIM AHT
ECOP LiBr AHT
ECOP EMIM AHT

b)

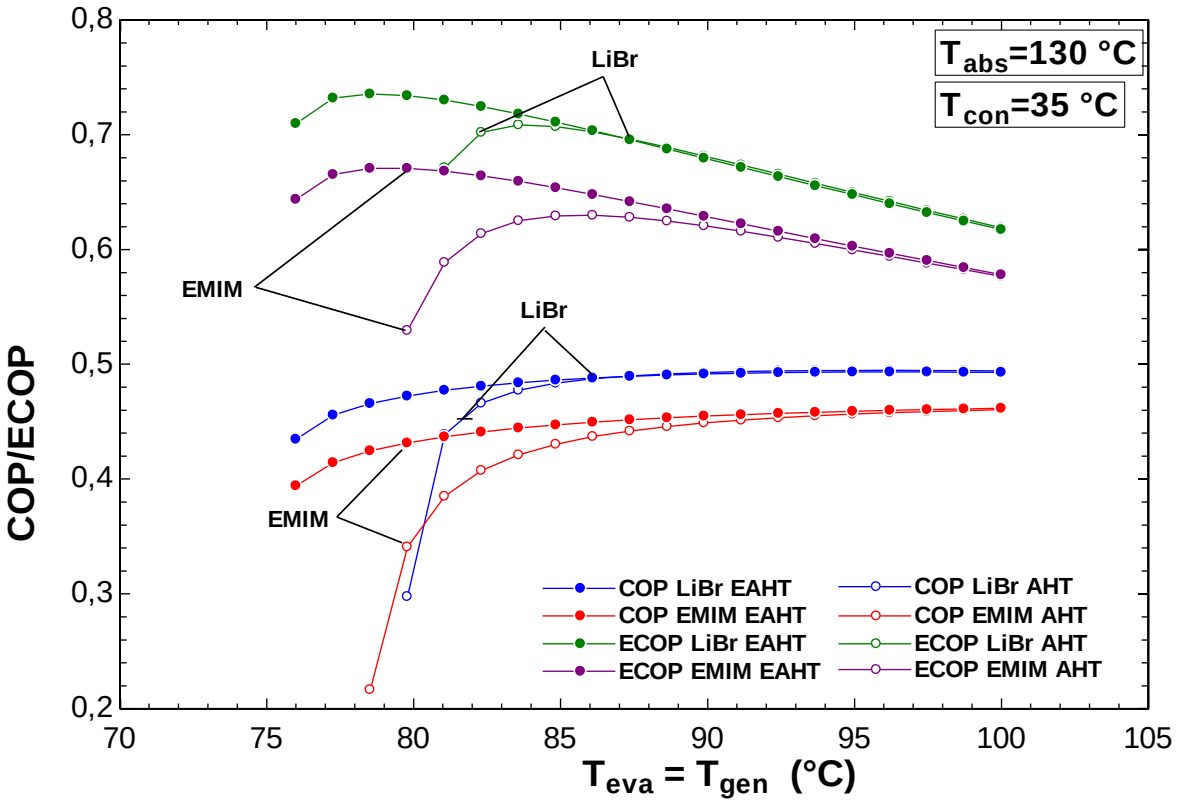
T_{abs}=130 °C
T_{con}=35 °C
LiBr
EMIM
LiBr
EMIM
COP/ECOP
T_{eva} = T_{gen} (°C)
COP LiBr EAHT
COP EMIM EAHT
ECOP LiBr EAHT
ECOP EMIM EAHT
COP LiBr AHT
COP EMIM AHT
ECOP LiBr AHT
ECOP EMIM AHT

c)

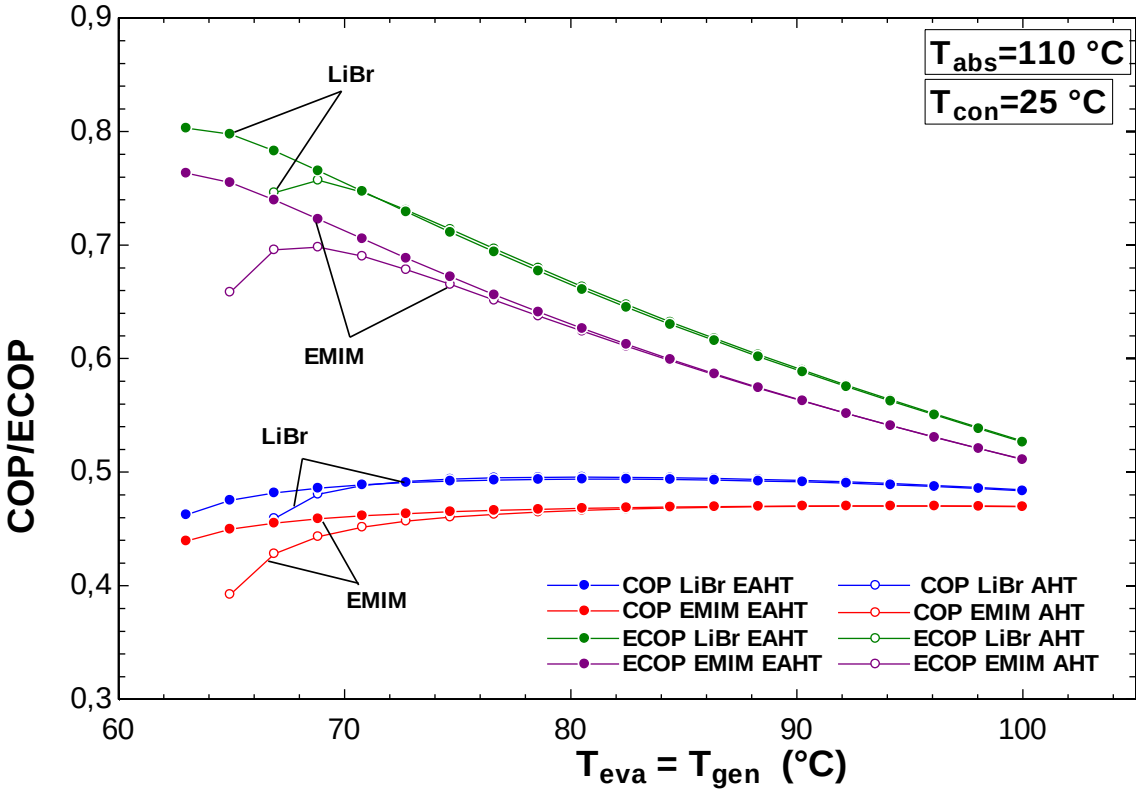

d)

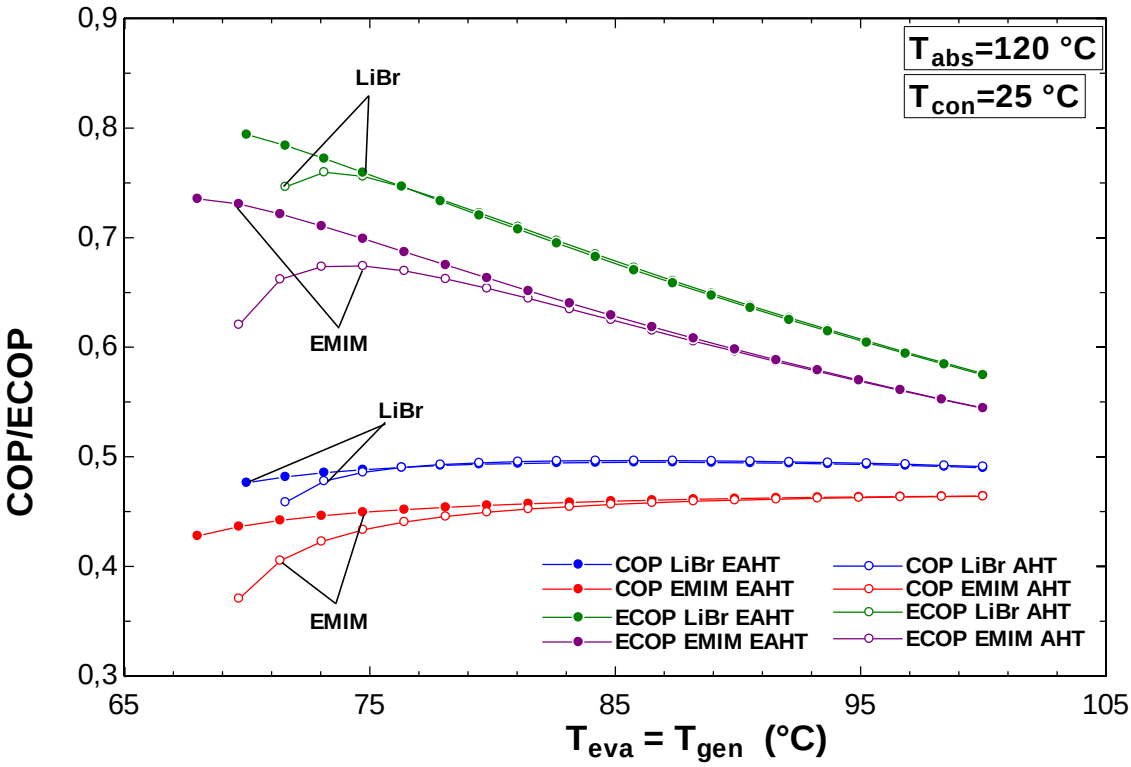

Figure 5.1 Effect of T_{gen} on COP and ECOP for both H_2O-LiBr and H_2O-[EMIM][DMP] cycles. (a) At T_{abs} = 120°C and T_{con} = 35°C. (b) At T_{abs} = 130°C and T_{con} = 35°C. (c) At T_{abs} = 110°C and T_{con} = 25°C. (d) At T_{abs} = 120°C and T_{con} = 25°C.

Table 5.2 Comparison of outputs of both systems with and without ejector at defined input parameters

		System 1 (H_2O-LiBr)		System 2 (H_2O-[EMIM][DMP])	
	Unit	**EAHT**	**AHT**	**EAHT**	**AHT**
Absorber temperature (T_{abs})	°C	135	135	135	135
Generator temperature (T_{gen})	°C	90	90	90	90
Evaporator temperature (T_{eva})	°C	90	90	90	90
Condenser temperature (T_{con})	°C	35	35	35	35
Flow ratio (f)	-	5.249	6.802	7.46	10.88
COP	-	0.4899	0.4903	0.4462	0.4354
ECOP	-	0.6975	0.698	0.6352	0.6199
Weak solution concentration (x_w)	-	0.544	0.5647	0.8173	0.8489
Strong solution concentration (x_s)	-	0.6477	0.6477	0.9269	0.9269
Absorber heat rate (Q_{abs})	kJ/kg	2422	2426	2031	1945
Generator heat rate (Q_{gen})	kJ/kg	2431	2435	2040	1954
Evaporator heat rate (Q_{eva})	kJ/kg	2513	2513	2513	2513
Condenser heat rate (Q_{con})	kJ/kg	2522	2522	2522	2522
Heat exchanger heat rate (Q_{eco})	kJ/kg	346	448.3	605.8	883.9

Reference operating conditions used are the input parameters in table 5.2. Here T_{abs} = **135°C**, T_{eva} = T_{gen} = 90°C and T_{con} = 35°C.

Table 5.3 State properties of the streams of the cycles at reference operating condition

Streams	Temperature (°K)	Pressure (kPa)	Mass flow rate (kg s^{-1})	Absorbent concentration (wt%)	Specific enthalpy (kJ kg^{-1})	Specific entropy (kJ kg^{-1})
H_2O-LiBr cycle						
1	363.2	5.642	1	-	2669	8.661
2	308.2	5.642	1	-	146.8	0.5056
3	308.2	70.25	1	-	146.9	0.5056
4	363.2	70.25	1	-	2660	7.478
5	408.2	70.25	7.802	0.5647	296.4	0.7823
6	381	70.25	7.802	0.5647	238.9	0.6376
7	348.2	5.642	7.802	0.5647	238.9	0.6482
8	363.2	5.642	6.802	0.6477	239.7	0.4754
9	363.2	70.25	6.802	0.6477	239.7	0.4754
10	399.2	70.25	6.802	0.6477	305.6	0.6484
H_2O-LiBr cycle with ejector						
1	363.2	5.642	1	-	2669	8.661
2	308.2	5.642	1	-	146.8	0.5056
3	308.2	70.25	1	-	146.9	0.5056
4	363.2	70.25	1	-	2660	7.478
5	408.2	81.84	6.249	0.544	294.7	0.8102
6	382.7	81.84	6.249	0.544	239.3	0.6711
7	344.4	5.642	6.249	0.544	239.3	0.6894
8	363.2	5.642	5.249	0.6477	239.7	0.4754
9	363.2	70.25	5.249	0.6477	239.7	0.4754
10	399.2	70.25	5.249	0.6477	305.6	0.6484
11	393.2	81.84	6.249	0.544	682.3	0.7291
H_2O-[EMIM][DMP] cycle						
1	363.2	5.642	1	-	2669	8.661
2	308.2	5.642	1	-	146.8	0.5056
3	308.2	70.25	1	-	146.9	0.5056
4	363.2	70.25	1	-	2660	7.478
5	408.2	70.25	11.88	0.8489	478.9	1.93
6	379.1	70.25	11.88	0.8489	404.5	1.748
7	-	5.642	11.88	0.8489	404.5	1.778
8	363.2	5.642	10.88	0.9269	376	1.634
9	363.2	70.25	10.88	0.9269	376	1.634
10	399.2	70.25	10.88	0.9269	457.2	1.84
H_2O-[EMIM][DMP] cycle with ejector						
1	363.2	5.642	1	-	2669	8.661
2	308.2	5.642	1	-	146.8	0.5056
3	308.2	70.25	1	-	146.9	0.5056
4	363.2	70.25	1	-	2660	7.478
5	408.2	89.41	8.46	0.8173	477.4	1.933
6	381.2	89.41	8.46	0.8173	405.8	1.758

7	-	5.642	8.46	0.8173	405.8	1.796
8	363.2	5.642	7.46	0.9269	376	1.634
9	363.2	70.25	7.46	0.9269	376	1.634
10	399.2	70.25	7.46	0.9269	457.2	1.84
11	395.9	89.41	8.46	0.8173	717.5	-

Figure 5.2 shows the effect of absorber temperature on the COP of system 1, comparing the cycle with and without ejector at various condenser temperatures, while the evaporator temperature is held at 90°C. For all the condenser temperatures, the COP initially increases early on before it starts to reduce. At T_{con}=25°C, COP is the highest and the decrease is the least severe. The higher the condenser temperature is, the lower COP becomes and the faster it decreases. Comparing the COP development of AHT against EAHT, it is observed that COP is higher for AHT at lower absorber temperatures. However, at a certain point the more rapid decrease in AHT COP leads to EAHT COP overtaking and remaining higher for the high absorber temperature range. As the condenser temperature increases, the overtaking occurs at lower absorber temperatures. At T_{con}=25°C a shift around T_{abs}=145°C is witnessed. At T_{con}=40°C the shift occurs at around T_{abs}=131°C. After the shift, the ejector addition contributes to an improved COP. At T_{con}=35°C and T_{abs}=152°C the COP of EAHT is 36.10% higher than the COP of AHT. This is the maximum point of COP increase between EAHT and AHT. As can also be observed from figure 5.2 that the ejector addition allows higher absorber temperatures at T_{con}=35 and 40°C. This is because of the lowered flow ratio caused by ejector addition, making it possible to push the maximum GTL higher.

This means the installation of ejector is only an improvement to COP and subsequently ECOP at higher absorber temperatures. The same effect for ECOP is seen in figure 5.3. Here, ECOP increases across most of the temperature range, before it starts declining and, in most cases, decreases. ECOP for all the condenser temperatures are lower for EAHT ECOP than AHT ECOP for most of the temperature range. At certain points the more rapid decline of AHT ECOP lead to EAHT ECOP surpassing it, leading to superior performance for EAHT. This decline is more rapid for higher condenser temperatures.

At lower condenser temperatures, both the COP and ECOP have higher quantities. The low condenser temperature increases the risk of LiBr crystallization. Therefore, it is important to control the input and output temperatures of the system at lower condenser temperatures to avoid crystallization. High condenser temperatures also lead to a more rapid turning point of decline, with the ECOP falling for T_{con}=40°C, compared to the absent decline of T_{con}=25°C. The observations of COP and exergy efficiency behaviour for LiBr are in agreement with Shi et al. [55].

For the COP and ECOP, the addition of an ejector only leads to performance improvement at higher absorber temperatures. The improved performance is noticeable for higher condenser temperatures, making ejector addition to improve the performance over a larger temperature range of these temperatures than for lower temperatures. The installation of an ejector will only be advantageous if the operator wishes to achieve high GTL for applications requiring such criteria. Being able to upgrade the heat to higher temperatures do increase the range of applications as discussed in the literature review. However, very high absorber temperatures result in very large heat losses to the environment in real applications. If GTL in the range of 50-75 °C is not necessary or economically feasible, then running the system without an ejector would be preferred in the case of H_2O-LiBr solution.

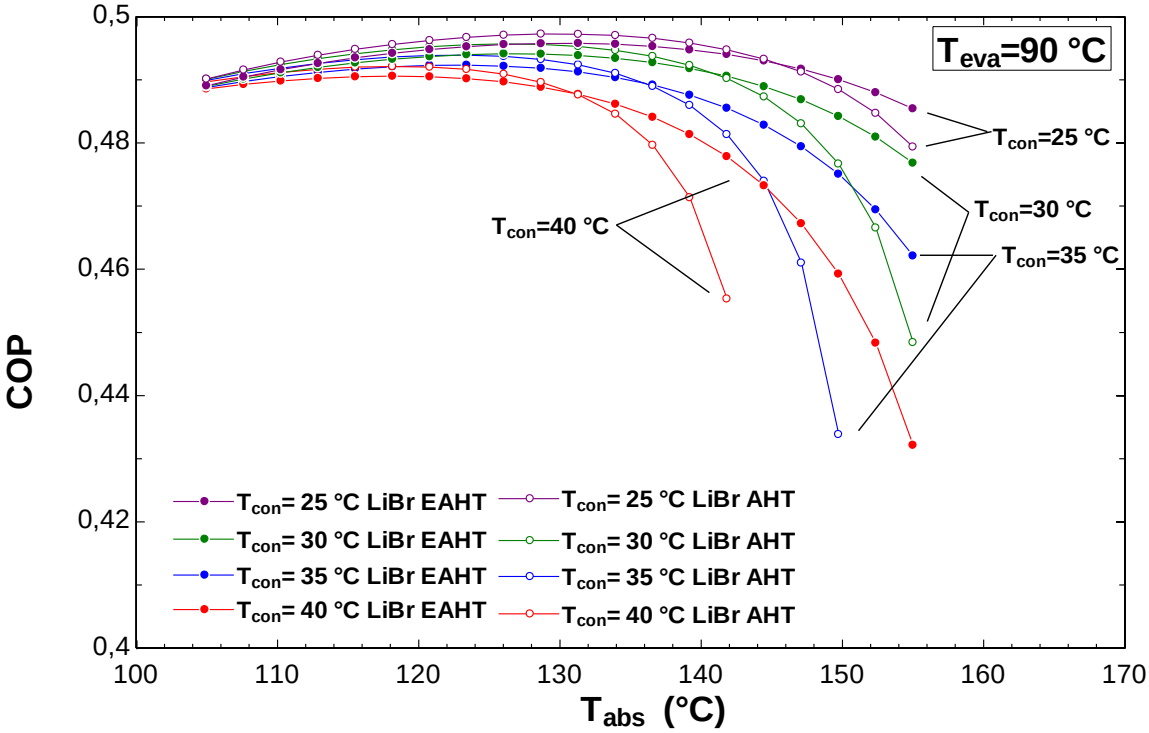

Figure 5.2 Effect of T_{abs} on COP for H_2O-LiBr cycle with and without ejector at various condenser temperatures.

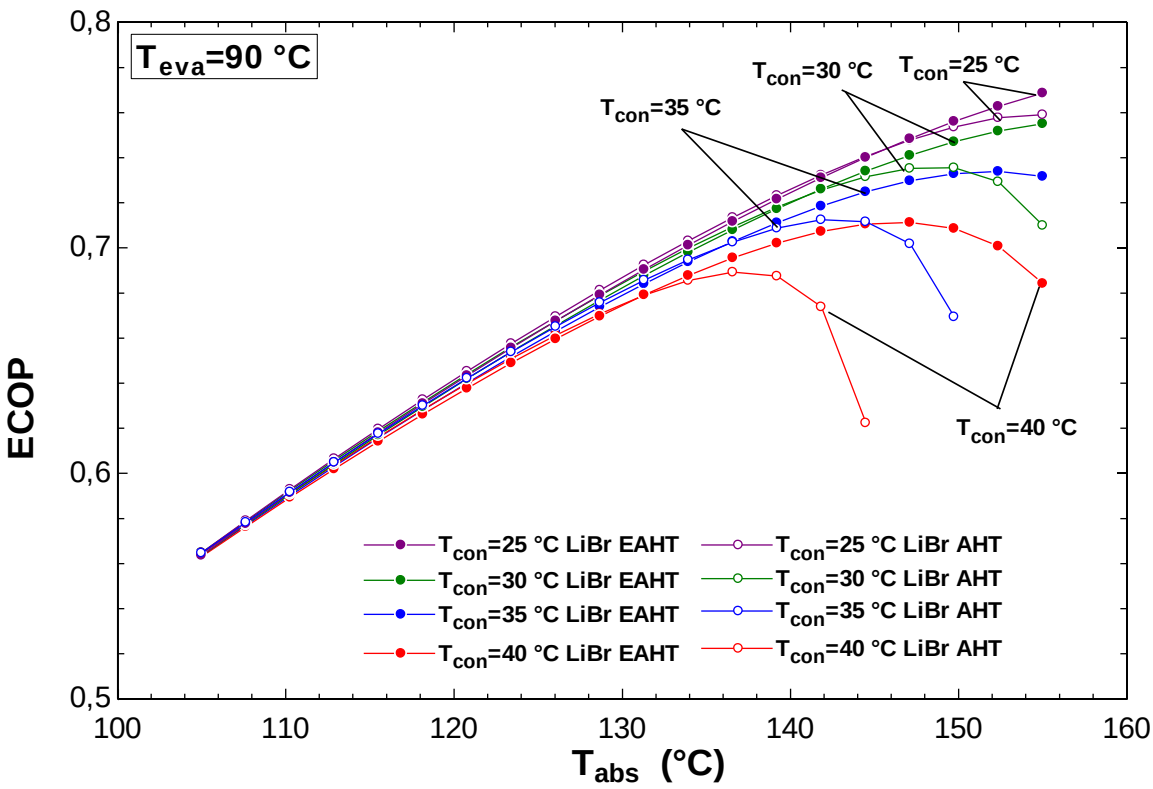

Figure 5.3 Effect of T_{abs} on ECOP for H_2O-LiBr cycle with and without ejector at various condenser temperatures.

Figure 5.4 shows the effect of absorber temperature on COP for system 2, comparing the cycle with and without ejector at various condenser temperatures when evaporator temperature is held at 90°C. For system 2 the behaviour of COP and ECOP is different compared to the behaviour of COP and ECOP of system 1. COP continuously declines across the temperature range for all condenser temperatures. The higher the condenser temperature is the more rapid the decline becomes. A major difference is observed with how AHT COP is only slightly higher than EAHT COP for absorber temperatures up to around 110°C for all four condenser temperatures. In addition to that, the ejector addition improves the COP, with the increase only growing as the temperature increases. For T_{con}=35°C and T_{abs}=129°C the ejector addition gives a COP increase of 1.08% and at T_{abs}=152°C the maximum COP increase of 75.75% is witnessed. Another interesting change from system 1 is that the higher condenser temperatures have higher COPs over the lower temperature range, only being surpassed at the end of the range of the lower condenser temperatures. The ejector addition now allows higher temperatures for all the 4 scenarios. The higher the condenser temperature is the higher the obtainable absorber temperature becomes. For T_{con}=25,30°C the maximum absorber temperature attainable is lower than of T_{con}=35,40°C. This makes using lower condenser temperatures not as good of an option if absorber temperatures higher than 140-150°C are desired. COP variations caused by condenser temperature are smaller for system 2 compared to system 1.

From figure 5.5 ECOP will follow COP behaviour in most regards, however, the development of it goes differently, with a steady increase going into a stagnation point before decline for T_{con}=30,35,40°C. The decline is much more rapid for higher condenser temperatures. Maximum attainable temperature is greatly improved by ejector for T_{con}=35,40°C. EAHT ECOP surpasses AHT ECOP early on, with large increases in performance at high absorber temperatures.

System 2 shows a better performance improvement by adding ejector, compared to system 1. Using H_2O-[EMIM][DMP] as the working fluid leads to performance improvement at all temperatures above approximately 110°C. The improvement is noticeable for higher condenser temperatures, where

ejector addition lead to both higher COP and ECOP increases, as well as extending the maximum temperatures attainable in the absorber. Unlike system 1, the installation of an ejector in system 2 will be advantageous for all temperatures above 110°C. The improvement is only a few percent in the lower ranges, and this improvement drastically increase in the range of 130-140°C in the absorber. It can be concluded that the EAHT for system 2 is a great addition with no drawbacks regarding the thermodynamic performance of the system.

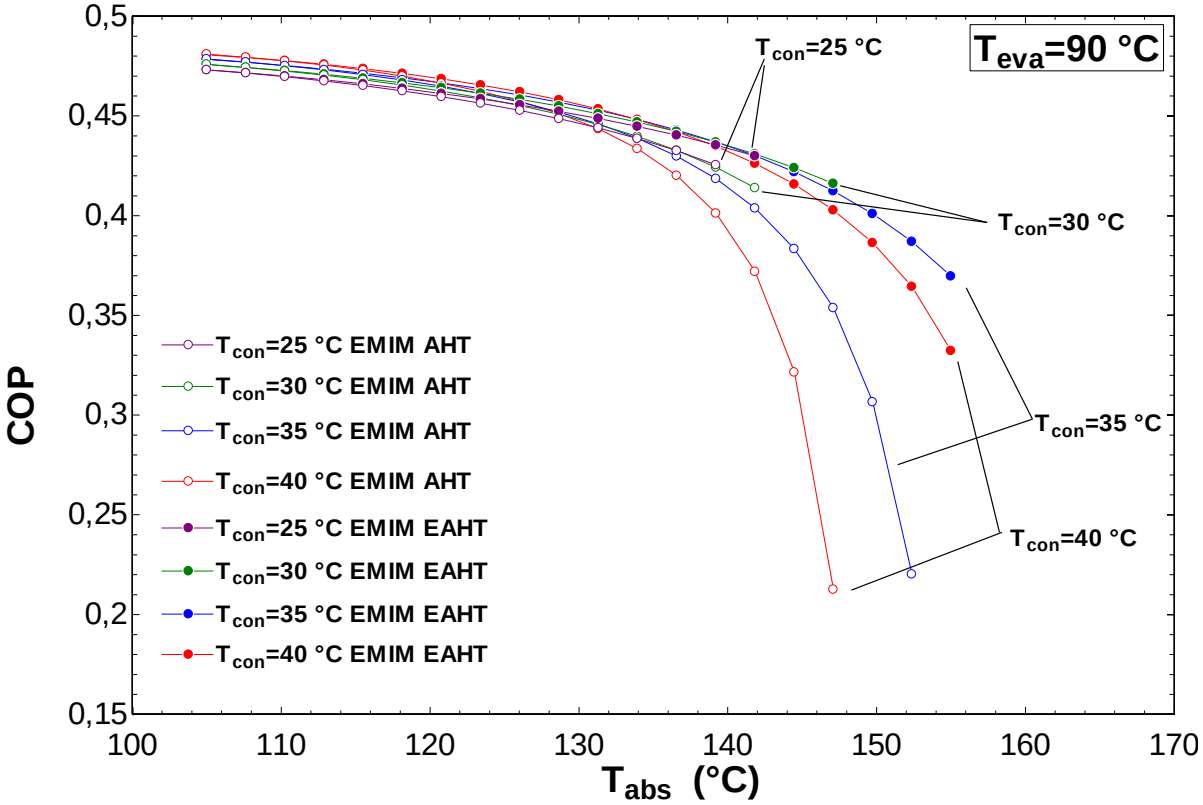

Figure 5.4 Effect of T_{abs} on COP for H_2O-[EMIM][DMP] cycle with and without ejector at various condenser temperatures.

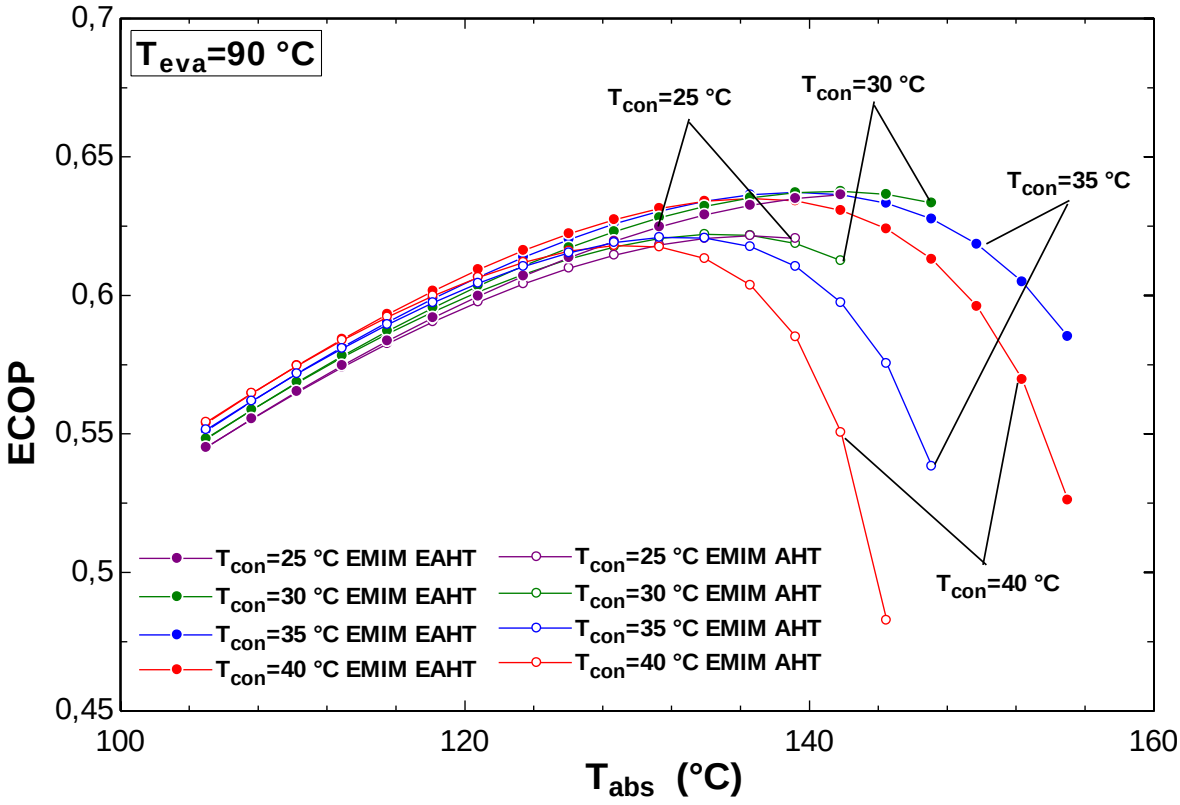

Figure 5.5 Effect of T_{abs} on ECOP for H_2O-[EMIM][DMP] cycle with and without ejector at various condenser temperatures.

Figure 5.6 and 5.7 represent the variation of COP as a function of absorber temperature at various evaporator temperatures for LiBr and [EMIM][DMP], respectively while the condenser temperature is fixed as 35°C. The addition of ejector extends the GTL of all three evaporator temperatures. The GTL is extended the most for T_{eva}=80°C in both the systems. The comparison of GTL between EAHT and AHT is listed on table 5.4 below. Adding an ejector does not change the comparative performance between the two working fluid pairs, that is H_2O-LiBr COP > H_2O-([EMIM][DMP]) COP for all evaporator temperatures. COP for system 2 still decreases at faster rate than that of COP for system 1. AHT COP and EAHT COP for system 1 stays approximately the same, with AHT COP being slightly higher for the lower temperature range, and EAHT COP overtaking it and remaining slightly higher before diverging due by a slower decline rate. For system 2 the AHT COP only remains higher at the lowest absorber temperatures, before EAHT COP overtakes it. The divergence of COP values happens much earlier and stretches over a longer range for system 2.

Table 5.4 GTL comparison between system with ejector and without ejector

	H_2O-LiBr (System 1)		**H_2O-([EMIM][DMP]) (System 2)**	
Evaporator temperature	EAHT	AHT	EAHT	AHT
T_{eva}=70°C	25	19	25	22
T_{eva}=80°C	50	39	50	43
T_{eva}=90°C	60	56	60	56

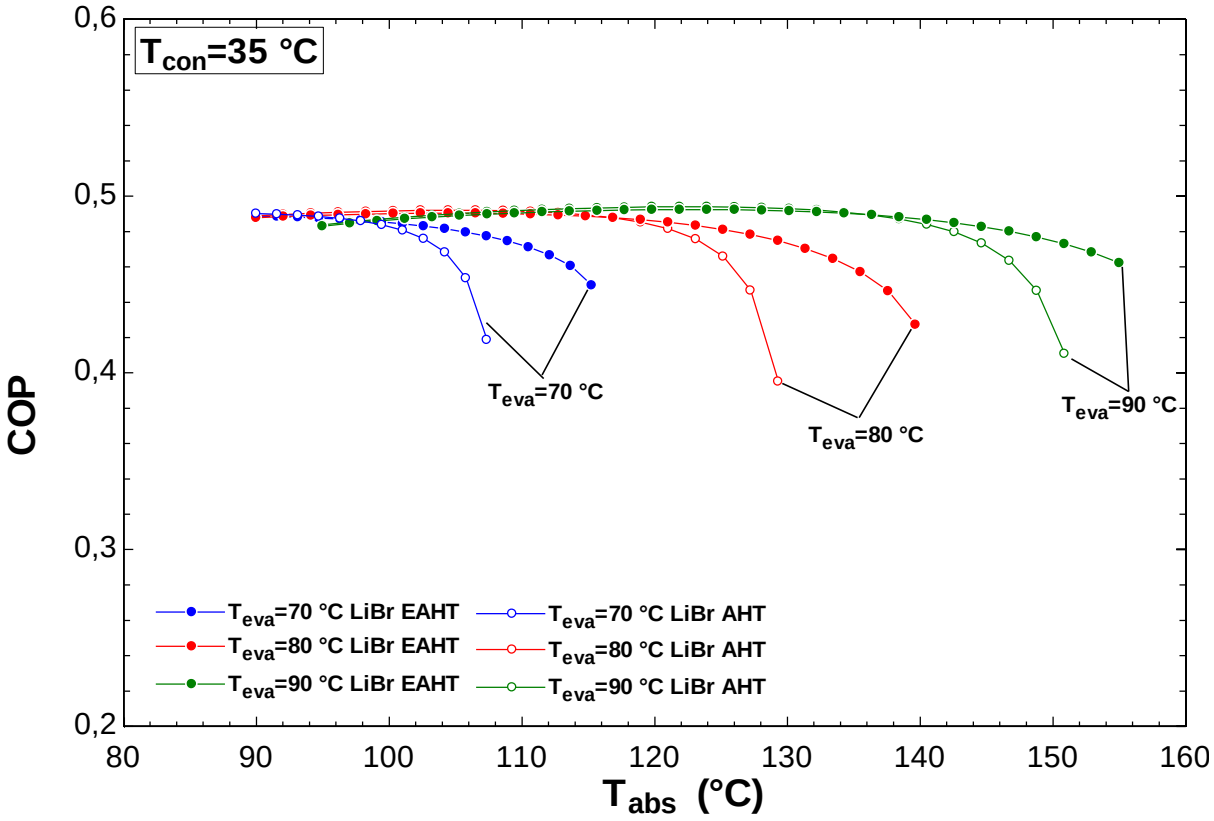

Figure 5.6 Effect of T_{abs} on COP for H_2O-LiBr cycle with and without ejector at various evaporator temperatures.

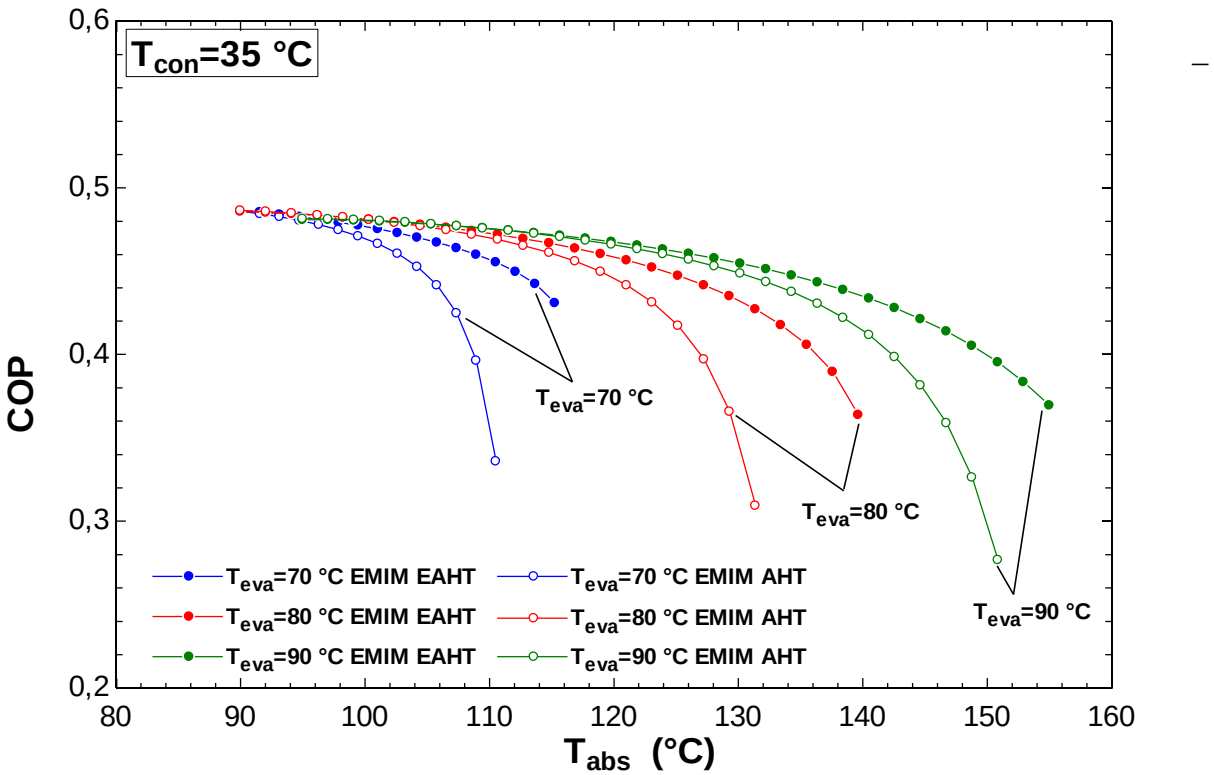

Figure 5.7 Effect of T_{abs} on COP for H_2O-[EMIM][DMP] cycle with and without ejector at various evaporator temperatures.

Figure 5.8 shows the effect of absorber temperature on the solution concentration difference, Δx and flow ratio, f for systems 1 and system 2. The evaporator and condenser temperatures are held at 90°C and 35°C, respectively. These are the two last important performance parameters that will be investigated. In both the cases, Δx difference between the EAHT and AHT increases across the temperature range, and is maximized at maximum temperature of T_{abs}=155°C. The difference of Δx is higher in system 2. As can be seen in table 5.2, the ejector addition does not affect the strong solution concentration, x_s. However, it makes the weak solution concentration, x_w, lower, increasing Δx. The increased Δx results in more driving force caused by mass transfer through both absorber and generator [34]. This is reflected on the flow ratio, f, in the same figures. As Δx decreases, the flow ratio increases and by higher Δx values, the flow ratio is lowered. A lower flow ratio is constructive for several reasons. A lower flow ratio saves capital expenditure (CAPEX) of the system, since it dictates the size of equipment. A higher flow ratio limit requires larger equipment which are costly. This means that there are effectively monetary restrictions on how the high flow ratio can become during operations. By lowering the flow ratio through an ejector addition, it is considerably more affordable to run operations at high absorber temperatures. Absorber temperature and Δx can be controlled through adjusting flow ratio. It is noted that EAHT flow ratio for system 2 remains higher than EAHT flow ratio for system 1 in the entire range. This is in contrast with flow ratios for AHT, where the flow ratio for system 1 surpasses system 2 at approximately T_{abs}=150°C. From purely economic terms, system 1 is a better choice when it comes to capital cost due to the lower flow ratio, and it has higher COP and ECOP values as well.

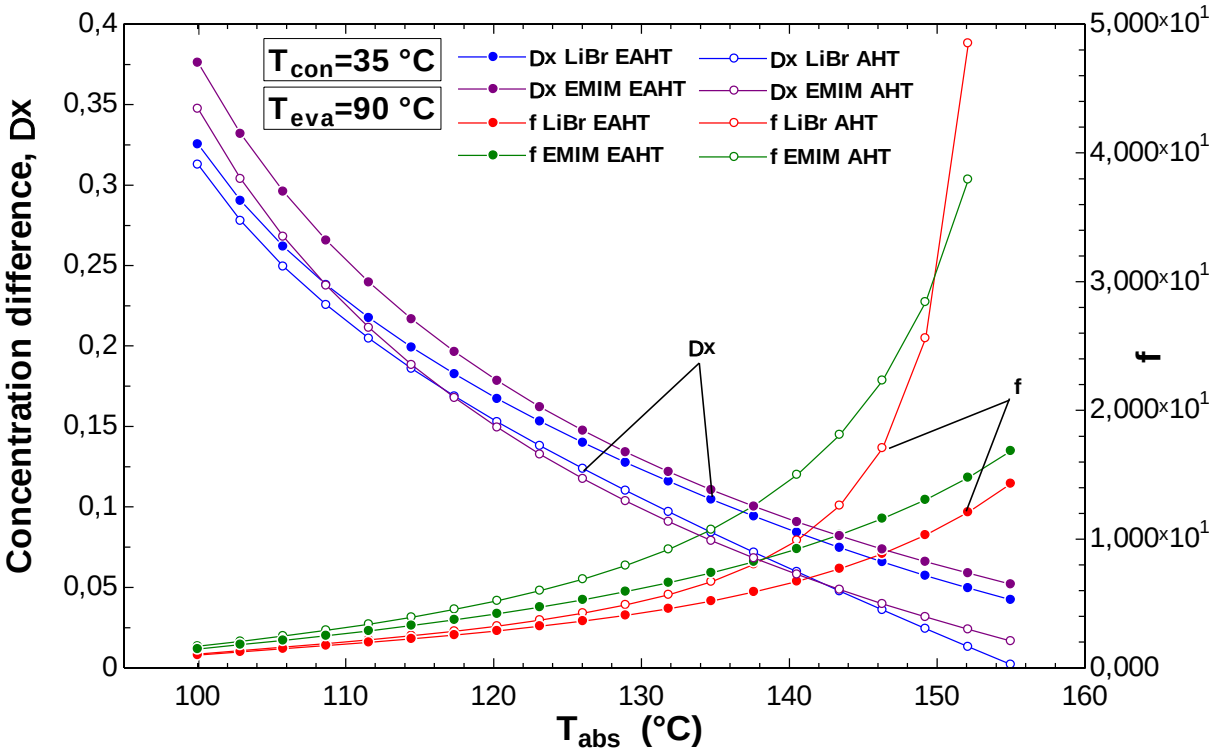

Figure 5.8 Effect of T_{abs} on Δx and flow ratio for H_2O-LiBr and H_2O-[EMIM][DMP].

Adding ejector does not affect LiBr crystallization in any direct way as Figure 5.9 show. Here, strong solution concentration as a function of generator temperature at four different condenser temperatures are plotted after ejector is added. The figure shows that the LiBr crystallization risk remains the same for system 1 as it did before ejector addition. The lower the condenser temperature, the higher the performance of the system is. At low condenser temperatures the risk of crystallization is higher. This is therefore a constriction that system 1 has, which is not found in system 2. System 2 using the ionic liquid [EMIM][DMP] as absorbent have no crystallization risk. This is one of the major advantages of using an ionic liquid over a salt. The same for System 2 has also been plotted in figure 5.9. The purpose is to show the much higher strong solution concentration demanded for the same operating parameters of system 1, there would be crystallization risk if system 1 was used, whereas there is no such risk for system 2. Despite what figure 5.9 demonstrates about LiBr crystallization risk, it is potentially lowered, should a lower generator temperature be used. As discussed earlier, the addition of an ejector allows for more effective utilization of the system at lower generator

temperatures. The lower the generator temperature is, the lower the risk of crystallization becomes. Therefore, installing an ejector can indirectly lower crystallization risk by having the system use lower-grade heat sources.

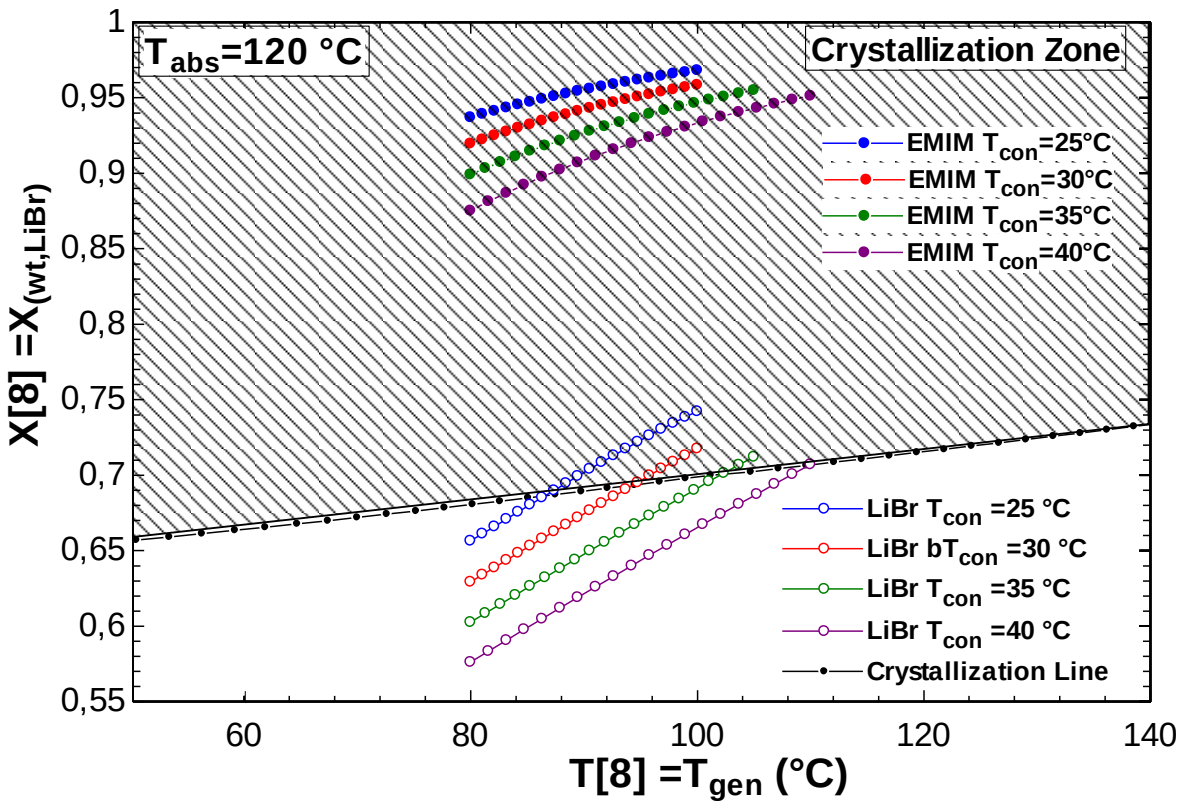

Figure 5.9 Effect of condenser and heat source temperature on H_2O-LiBr crystallization with ejector, compared against H_2O-[EMIM][DMP]. Original plot by Kamali et al. [34], modified by author for ejector and addition of system 2.

5 Conclusion

The performance of adding an ejector at the absorber inlet of a single-stage absorption heat transformer, using H_2O-LiBr and H_2O-[EMIM][DMP] as the working fluids have been investigated. It was found that using an ejector at the absorber inlet of both H_2O-LiBr and H_2O-[EMIM][DMP] absorption heat transformer cycles improves their performances. Due to the addition of ejector the absorber pressure is slightly higher and there is better mixing between the strong solution and the refrigerant vapour. The simulations carried out in EES show that for H_2O-LiBr the COP and ECOP as functions of T_{gen} are improved at lower generator temperature but remains equal or just slightly lower for the rest of the range. H_2O-[EMIM][DMP] performs better, with improved COP and ECOP over a longer range of temperatures. Ejector addition enables more effective utilization of low-grade heat. EAHT also start operating at lower temperatures for both the systems. Operating at lower generator temperatures also lowers the crystallization risk of system 1.

COP and ECOP as functions of T_{abs} for all the operating conditions investigated are improved at higher absorber temperatures. H_2O-LiBr performs worse at lower temperatures, gaining only an increase in the performance of the upper end of the temperature range investigated. H_2O-[EMIM][DMP] again performs better, with improvements in COP and ECOP starting between 105-110°C. At T_{con}=35°C and T_{abs}=152°C, the maximum COP improvement is found to be 36.10% for system 1. In contrast, the maximum COP improvement for system 2 at the same temperatures is 75.75%. Overall, system 2 benefits the most from ejector addition.

GTLs are improved by the ejector addition for all operating conditions investigated. System 1 showed the largest GTL improvement. Solution concentration difference Δx increased for both the systems, and flow ratios decreased. LiBr crystallization is not affected by ejector addition directly. To conclude, the addition of ejector will be mostly beneficial to system 2. System 1 performs worse with ejector at lower absorber temperatures, while system 2 has significant performance improvement everywhere but the lowest absorber temperatures. Installing ejector for system 1 is recommended if lower-grade

heat sources are to be utilized, or if very high absorber temperatures are sought after. For system 2, ejector addition is thoroughly recommended for improving performance for all conditions.

References

1. Rivera, W., M.J. Cardoso, and R.J. Romero, *Single-stage and advanced absorption heat transformers operating with lithium bromide mixtures used to increase solar pond's temperature.* Solar Energy Materials and Solar Cells, 2001. **70**(3): p. 321-333.
2. Ma, X., et al., *Application of absorption heat transformer to recover waste heat from a synthetic rubber plant.* Applied Thermal Engineering, 2003. **23**(7): p. 797-806.
3. Al-Alili, A., et al., *Modeling of a solar powered absorption cycle for Abu Dhabi.* Applied Energy, 2012. **93**: p. 160-167.
4. Srikhirin, P., S. Aphornratana, and S. Chungpaibulpatana, *A review of absorption refrigeration technologies.* Renewable and Sustainable Energy Reviews, 2001. **5**(4): p. 343-372.
5. Táboas, F., M. Bourouis, and M. Vallès, *Analysis of ammonia/water and ammonia/salt mixture absorption cycles for refrigeration purposes in fishing ships.* Applied Thermal Engineering, 2014. **66**(1): p. 603-611.
6. Zhang, N. and N. Lior, *Development of a novel combined absorption cycle for power generation and refrigeration1.* Journal of Energy Resources Technology, Transactions of the ASME, 2007. **129**(3): p. 254-265.
7. Ayou, D.S., et al., *Analysis and simulation of modified ammonia/water absorption cycle for power and cooling applications.* International Journal of Low-Carbon Technologies, 2013. **8**: p. i19-i26.
8. Ababneh, A., *Energy conservation using a double-effect absorption cycle driven by solar energy and fossil fuel*. Vol. 5. 2011. 213-219.
9. Lin, P., et al., *Ammonia-water absorption cycle: A prospective way to transport low-grade heat energy over long distance.* International Journal of Low-Carbon Technologies, 2011. **6**(2): p. 125-133.
10. Yosaf, S. and H. Ozcan, *Exergoeconomic investigation of flue gas driven ejector absorption power system integrated with PEM electrolyser for hydrogen generation.* Energy, 2018. **163**: p. 88-99.
11. Alexis, G.K. and E.D. Rogdakis, *Performance of solar driven methanol–water combined ejector–absorption cycle in the Athens area.* Renewable Energy, 2002. **25**(2): p. 249-266.
12. Bellos, E. and C. Tzivanidis, *Parametric analysis and optimization of a cooling system with ejector-absorption chiller powered by solar parabolic trough collectors.* Energy Conversion and Management, 2018. **168**: p. 329-342.
13. Wang, J., G. Chen, and H. Jiang, *Study on a solar-driven ejection absorption refrigeration cycle.* International Journal of Energy Research, 1998. **22**(8): p. 733-739.
14. Wang, D., et al., *Post combustion CO2 capture in power plant using low temperature steam upgraded by double absorption heat transformer.* Applied Energy, 2018. **227**: p. 603-612.
15. Parham, K., et al., *Comparative assessment of different categories of absorption heat transformers in water desalination process.* Desalination, 2016. **396**: p. 17-29.
16. Sekar, S. and R. Saravanan, *Experimental studies on absorption heat transformer coupled distillation system.* Desalination, 2011. **274**(1): p. 292-301.
17. Horuz, I. and B. Kurt, *Absorption heat transformers and an industrial application.* Renewable Energy, 2010. **35**(10): p. 2175-2181.
18. Horuz, I. and B. Kurt, *Single stage and double absorption heat transformers in an industrial application.* International Journal of Energy Research, 2009. **33**(9): p. 787-798.
19. Parham, K., et al., *Absorption heat transformers - A comprehensive review.* Renewable and Sustainable Energy Reviews, 2014. **34**: p. 430-452.
20. Rivera, W., et al., *A review of absorption heat transformers.* Applied Thermal Engineering, 2015. **91**: p. 654-670.
21. Donnellan, P., K. Cronin, and E. Byrne, *Recycling waste heat energy using vapour absorption heat transformers: A review.* Renewable and Sustainable Energy Reviews, 2015. **42**: p. 1290-1304.

22. Stephan, K. and D. Seher, *Heat transformer cycles—II. Thermodynamic analysis and optimization of a single-stage absorption heat transformer.* Journal of Heat Recovery Systems, 1984. **4**(5): p. 371-375.
23. Eisa, M.A.R., R. Best, and F.A. Holland, *Thermodynamic design data for absorption heat transformers-part I. Operating on water-lithium bromide.* Journal of Heat Recovery Systems, 1986. **6**(5): p. 421-432.
24. Rivera, W., et al., *Experimental assessment of double-absorption heat transformer operating with H2O/LiBr.* Applied Thermal Engineering, 2018. **132**: p. 432-440.
25. Donnellan, P., et al., *First and second law multidimensional analysis of a triple absorption heat transformer (TAHT).* Applied Energy, 2014. **113**: p. 141-151.
26. Rivera, W., et al., *Thermodynamic study of advanced absorption heat transformers—I. Single and two stage configurations with heat exchangers.* Heat Recovery Systems and CHP, 1994. **14**(2): p. 173-183.
27. Rivera, W., et al., *Thermodynamic study of advanced absorption heat transformers—II. Double absorption configurations.* Heat Recovery Systems and CHP, 1994. **14**(2): p. 185-193.
28. Hong, S.J., et al., *Analysis of single stage steam generating absorption heat transformer.* Applied Thermal Engineering, 2018. **144**: p. 1109-1116.
29. Fartaj, S.A., *Comparison of energy, exergy, and entropy balance methods for analysing double-stage absorption heat transformer cycles.* International Journal of Energy Research, 2004. **28**(14): p. 1219-1230.
30. Wang, L., et al., *Performance Study of a Double Absorption Heat Transformer.* Energy Procedia, 2017. **105**: p. 1473-1482.
31. Colorado, D., et al., *Irreversibility analysis of the absorption heat transformer coupled to a single effect evaporation process.* Applied Thermal Engineering, 2016. **92**: p. 71-80.
32. Kurem, E. and I. Horuz, *A comparison between ammonia-water and water-lithium bromide solutions in absorption heat transformers.* International Communications in Heat and Mass Transfer, 2001. **28**(3): p. 427-438.
33. Salehi, S., et al., *Investigation of crystallization risk in different types of absorption LiBr/H2O heat transformers.* Thermal Science and Engineering Progress, 2019. **10**: p. 48-58.
34. Kamali, M., K. Parham, and M. Assadi, *Performance analysis of a single stage absorption heat transformer-based desalination system employing a new working pair of (EMIM) (DMP)/H2O.* International Journal of Energy Research, 2018. **42**(15): p. 4790-4804.
35. Goerge, J.M. and S. Srinivasa Murthy, *Experiments on a vapour absorption heat transformer: Expériences sur un transformateur de chaleur à absorption de vapeur.* International Journal of Refrigeration, 1993. **16**(2): p. 107-119.
36. Fatouh, M. and S. Srinivasa Murthy, *Comparison of R22-absorbent pairs for vapour absorption heat transformers based on P-T-X-H data.* Heat Recovery Systems and CHP, 1993. **13**(1): p. 33-48.
37. Ciambelli, P. and V. Tufano, *The upgrading of waste heat by means of water-sulphuric acid absorption heat transformers.* Heat Recovery Systems and CHP, 1987. **7**(6): p. 517-524.
38. Zhuo, C.Z. and C.H.M. Machielsen, *Performance of high-temperature absorption heat transformers using Alkitrate as the working pair.* Applied Thermal Engineering, 1996. **16**(3): p. 255-262.
39. Best, R. and W. Rivera, *Thermodynamic design data for absorption heat transformers. Part six: Operating on water-carrol.* Heat Recovery Systems and CHP, 1994. **14**(4): p. 427-436.
40. Best, R., et al., *Modelling of single-stage and advanced absorption heat transformers operating with the water/carrol mixture.* Applied Thermal Engineering, 1997. **17**(11): p. 1111-1122.
41. Rivera, M.W., M.J. Cardoso, and R.J. Romero, *Theoretical comparison of single stage and advanced absorption heat transformers operating with water/lithium bromide and water/carrol.* International Journal of Energy Research, 1998. **22**(5): p. 427-442.

42. Sotelo, S.S. and R.J. Romero, *Improvement of recovery energy in the absorption heat transformer process using water - Carrol™ for steam generation.* Chemical Engineering Transactions, 2009. **17**: p. 317-322.
43. Yin, J., et al., *Performance analysis of an absorption heat transformer with different working fluid combinations.* Applied Energy, 2000. **67**(3): p. 281-292.
44. Zhuo, C.Z. and C.H.M. Machielsen, *Thermodynamic assessment of an absorption heat transformer with TFE-Pyr as the working pair.* Heat Recovery Systems and CHP, 1994. **14**(3): p. 265-272.
45. Zhao, Z., X. Zhang, and X. Ma, *Thermodynamic performance of a double-effect absorption heat-transformer using TFE/E181 as the working fluid.* Applied Energy, 2005. **82**(2): p. 107-116.
46. Barracan, R.M., et al., *Experimental performance of ternary solutions in an absorption heat transformer.* International Journal of Energy Research, 1998. **22**(1): p. 73-83.
47. Zhang, X. and D. Hu, *Performance analysis of the single-stage absorption heat transformer using a new working pair composed of ionic liquid and water.* Applied Thermal Engineering, 2012. **37**: p. 129-135.
48. Zhang, X., D. Hu, and Z. Zhao, *Thermodynamic performance of absorption heat transformer using a new working pair: Water+ionic liquid 1,3-dimethylimidazolium dimethylphosphate*, in *Advanced Materials Research*. 2012. p. 1258-1262.
49. Ayou, D.S., et al., *Performance analysis of absorption heat transformer cycles using ionic liquids based on imidazolium cation as absorbents with 2,2,2-trifluoroethanol as refrigerant.* Energy Conversion and Management, 2014. **84**: p. 512-523.
50. Abumandour, E.-S., F. Mutelet, and D. Alonso, *Performance of an absorption heat transformer using new working binary systems composed of {ionic liquid and water}.* Applied Thermal Engineering, 2016. **94**: p. 579-589.
51. Wang, M. and C.A. Infante Ferreira, *Absorption heat pump cycles with NH3 – ionic liquid working pairs.* Applied Energy, 2017. **204**: p. 819-830.
52. Sujatha, I. and G. Venkatarathnam, *Performance of a vapour absorption heat transformer operating with ionic liquids and ammonia.* Energy, 2017. **141**: p. 924-936.
53. Merkel, N., et al., *Operation of an absorption heat transformer using water/ionic liquid as working fluid.* Applied Thermal Engineering, 2018. **131**: p. 370-380.
54. Chen, W. and S. Liang, *Thermodynamic analysis of absorption heat transformers using [mmim]DMP/H2O and [mmim]DMP/CH3OH as working fluids.* Applied Thermal Engineering, 2016. **99**: p. 846-856.
55. Shi, L., et al., *Study on a new ejection–absorption heat transformer.* Applied Energy, 2001. **68**(2): p. 161-171.
56. Sözen, A., et al., *Performance parameters of an ejector-absorption heat transformer.* Applied Energy, 2005. **80**(3): p. 273-289.
57. Sözen, A. and H.S. Yücesu, *Performance improvement of absorption heat transformer.* Renewable Energy, 2007. **32**(2): p. 267-284.
58. Sun, D.-W., I.W. Eames, and S. Aphornratana, *Evaluation of a novel combined ejector-absorption refrigeration cycle — I: computer simulation.* International Journal of Refrigeration, 1996. **19**(3): p. 172-180.
59. Aphornratana, S. and I.W. Eames, *Experimental investigation of a combined ejector-absorption refrigerator.* International Journal of Energy Research, 1998. **22**(3): p. 195-207.
60. Wang, J., et al., *Parametric analysis for a new combined power and ejector–absorption refrigeration cycle.* Energy, 2009. **34**(10): p. 1587-1593.
61. Vereda, C., et al., *Study of an ejector-absorption refrigeration cycle with an adaptable ejector nozzle for different working conditions.* Applied Energy, 2012. **97**: p. 305-312.
62. Garousi Farshi, L., et al., *Thermodynamic analysis and comparison of combined ejector–absorption and single effect absorption refrigeration systems.* Applied Energy, 2014. **133**: p. 335-346.

63. Li, K., et al., *Thermodynamic analysis of a novel exhaust heat-driven non-adiabatic ejection-absorption refrigeration cycle using R290/oil mixture.* Energy Conversion and Management, 2017. **149**: p. 244-253.
64. Sözen, A. and E. Arcaklioğlu, *Exergy analysis of an ejector-absorption heat transformer using artificial neural network approach.* Applied Thermal Engineering, 2007. **27**(2): p. 481-491.
65. Chen, L.T., *A new ejector-absorber cycle to improve the COP of an absorption refrigeration system.* Applied Energy, 1988. **30**(1): p. 37-51.
66. Romero, R.J. and A. Rodríguez-Martínez, *Optimal water purification using low grade waste heat in an absorption heat transformer.* Desalination, 2008. **220**(1): p. 506-513.
67. Gomri, R., *Thermal seawater desalination: Possibilities of using single effect and double effect absorption heat transformer systems.* Desalination, 2010. **253**(1): p. 112-118.
68. Gomri, R., *Energy and exergy analyses of seawater desalination system integrated in a solar heat transformer.* Desalination, 2009. **249**(1): p. 188-196.
69. Huicochea, A., et al., *A novel cogeneration system: A proton exchange membrane fuel cell coupled to a heat transformer.* Applied Thermal Engineering, 2013. **50**(2): p. 1530-1535.
70. Aly, G., K. Abrahamsson, and Å. Jernqvist, *Application of absorption heat transformers for energy conservation in the oleochemical industry.* International Journal of Energy Research, 1993. **17**(7): p. 571-582.
71. Currie, J.S. and C.L. Pritchard, *Energy recovery and plume reduction from an industrial spray drying unit using an absorption heat transformer.* Heat Recovery Systems and CHP, 1994. **14**(3): p. 239-248.
72. Yang, S., et al., *Low grade waste heat recovery with a novel cascade absorption heat transformer.* Energy, 2017. **130**: p. 461-472.
73. Yang, S., et al., *A novel cascade absorption heat transformer process using low grade waste heat and its application to coal to synthetic natural gas.* Applied Energy, 2017. **202**: p. 42-52.
74. Gong, Y.-h., et al., *Viscosity and Density Measurements for Six Binary Mixtures of Water (Methanol or Ethanol) with an Ionic Liquid ([BMIM][DMP] or [EMIM][DMP]) at Atmospheric Pressure in the Temperature Range of (293.15 to 333.15) K.* Journal of Chemical & Engineering Data, 2012. **57**(1): p. 33-39.